JOC The Journal of Organic Chemistry

Note

pubs.acs.org/joc

Influence of 2′-Fluoro versus 2′-*O*-Methyl Substituent on the Sugar Puckering of 4′-*C*-Aminomethyluridine

Kiran R. Gore,[†] S. Harikrishna,[†] and P. I. Pradeepkumar*

Department of Chemistry, Indian Institute of Technology Bombay, Mumbai 400076, India

Supporting Information

ABSTRACT: Herein, we report the synthesis of 4′-*C*-aminomethyl-2′-deoxy-2′-fluorouridine, a therapeutically appealing RNA modification. Conformational analysis by DFT calculations and molecular dynamics simulations using trinucleotide model systems revealed that modified sugar adopts C3′-endo conformation. In this conformer, a weak intramolecular C−H···F H-bond between the hydrogen atom of the 4′-*C*-CH_2 group and the F atom at the 2′ position is observed. Comparative studies with unmodified, 2′-fluoro-, 2′-*O*-methyl-, and 4′-*C*-aminomethyl-2′-*O*-methyl-uridine showed the chemical nature of 2′-substituent dictates the sugar puckering of 2′,4′-modified nucleotides.

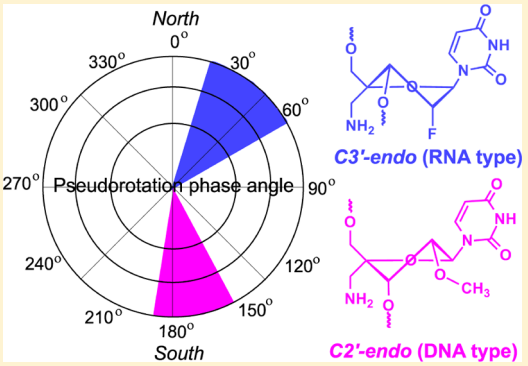

Various chemical modifications on the sugar moiety of nucleotides have been reported to improve the therapeutic potential of nucleic acids such as antisense oligonucleotides (AONs), aptamers, and small interfering RNAs (siRNAs).[1−5] However, the chemical nature of modifications play a crucial role in retaining the functional efficacy of these agents.[3−5] Among the plethora of sugar modifications reported, nucleic acids bearing a 2′-deoxy-2′-fluorine (2′-F) modification locks the sugar conformation in C3′-endo, increases the duplex stability, and enhances nuclease resistance properties of modified nucleic acids to a certain extent.[6−8] Combining the 2′-F along with other sugar modifications such as 4′-*C*-aminomethyl or 4′-thio is an attractive strategy to further improve the therapeutic properties of nucleic acids, in particular, the nuclease resistance.[9−11]

Chemical modifications in the furanose ring strongly influence the sugar puckering and the overall structure and stability of nucleic acids.[12] Like 2′-F,[6,7] C2′-modifications such as 2′-*O*-methyl (2′-OMe),[13,14] 2′-*O*-methoxyethyl (2′-MOE),[14,15] 2′-azido,[16] etc., tune the sugar toward the C3′-endo and stabilize both DNA/RNA and RNA/RNA duplexes. However, 2′-deoxy-2′-F-arabino nucleic acid (2′-F-ANA) modification adopts the O4′-endo conformation and renders moderate stability to duplexes.[17] Nucleic acids containing 4′-carbon bridged to 2′-carbon as in C3′-endo-fused locked nucleic acid (LNA) and carbocyclic LNA (c-LNA) show the largest RNA binding affinity.[18,19]

Toward the goal of harnessing the utilities of bifunctional sugar modifications, recently we have reported 4′-*C*-aminomethyl-2′-*O*-methyl (4′-AM-2′-OMe) uridine- and cytidine-modified siRNAs and 4′-AM-2′-OMe-thymidine triphosphate for potential applications in in vitro selection experiments.[20,21] The modified siRNAs showed significant enhancement in nuclease stability without compromising much in RNAi activity. However, the presence of this modification in an RNA duplex in general decreases the binding affinity (ΔT_m ~1 °C/modification) by favoring the C2′-endo conformation, which was elucidated by molecular dynamics (MD) simulations.[20] These studies clearly illustrate that the conformational pre-organization of the sugar influences the H-bonding and stacking interactions between nucleobases.[22] In this context, synthesis and conformational analysis of novel sugar-modified nucleosides can provide new insights for the design of therapeutically appealing nucleic acids.

Herein, we report the synthesis of 4′-*C*-aminomethyl-2′-deoxy-2′-fluoro (4′-AM-2′-F) uridine nucleoside (**D**) shown in Figure 1. The nature of sugar puckering and the Watson−Crick H-bonding of 4′-AM-2′-F-U in a trinucleotide model system were examined by DFT calculations, MD simulations, and utilizing umbrella sampling simulations. To distinguish the effect of 2′-modification from that of 4′-modification, comparative studies were also performed by using 2′-OH, 2′-OMe, 2′-F and 4′-AM-2′-OMe uridine (Figure 1) modified nucleotides.

Synthesis of 4′-AM-2′-F nucleoside **8** was achieved from uridine nucleoside **1**[20] as shown in Scheme 1. Deacetylation of **1** was carried out using sodium methoxide in methanol to get crude compound **2**. Nucleoside **2** was directly mesylated using methanesulfonyl chloride (Ms-Cl) in pyridine to afford mesylated nucleoside **3** in 80% yield (after two steps from **1**).[23] Treatment of **3** with aqueous NaOH gave arabinonucleoside **4** in 91% yield.[11] 2′-Fluorination of compound **4** using fluorinating agents such as (diethylamino)sulfur trifluoride

Received: June 12, 2013
Published: September 9, 2013

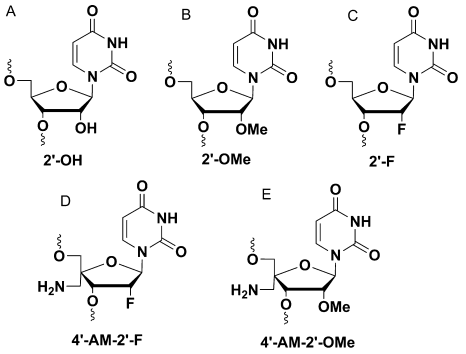

Figure 1. Structure of unmodified and modified uridine units: (A) 2′-hydroxyl (2′-OH), (B) 2′-*O*-methyl (2′-OMe), (C) 2′-fluoro (2′-F), (D) 4′-*C*-aminomethyl-2′-deoxy-2′-fluoro (4′-AM-2′-F), and (E) 4′-*C*-aminomethyl-2′-*O*-methyl (4′-AM-2′-OMe) .

(DAST) and [bis(2-methoxyethyl)amino]sulfur trifluoride (MAST), under different reaction conditions, led to decomposition of starting nucleoside.[24,25] To introduce an F atom at the 2′-position, arabino compound **4** was converted to its triflate **5** and then subsequently displaced by $Et_3N{\cdot}3HF$ in toluene at 45 °C to give the fluorinated nucleoside **6** in 45% yield.[26] Removal of benzyl groups, using 1 M BCl_3 in DCM by stirring at −78 to −30 °C, yielded the desired compound **7** in 83% yield.[27] Reduction of azide group of **7** with PPh_3 and H_2O in THF resulted in desired amine nucleoside **8** in 76% yield.[28]

Having achieved the synthesis of 4′-AM-2′-F-U, the sugar conformation adopted by the nucleoside in solution was studied by utilizing NMR coupling constants and PSEUROT program.[29] A population distribution of sugar conformation showed the modified nucleoside strongly prefers C3′-endo (>90%) with a pseudorotational phase angle (P) of 3−21° and puckering amplitude (φ_m) of 15−41° (Figure S1, Supporting Information). Since the results emerge from the conformational analysis using just modified nucleosides can be different from the corresponding modified nucleotides,[20,30] DFT calculations were performed in both gas phase (MP2/6-311++G*)[31] and in solvent (water) phase (PBE/6-311++G*)[32] using a model system where the modified nucleoside in the middle protected with sugar-phosphate moieties at the 3′- and 5′-ends (Figure S2, Supporting Information). When the conformational search was performed, sugars at both ends were fixed at C3′-endo puckering. In the solvent phase, calculations resulted in total 720 conformations for each modification. The lowest energy conformers of 2′-OMe, 2′-F, and 4′-AM-2′-F adopt P values in the range of 9−28° that correspond to the C3′-endo conformation, which is usually found in A-type RNA (Figure 2).[30,33] However, 4′-AM-2′-OMe-U showed lower energy

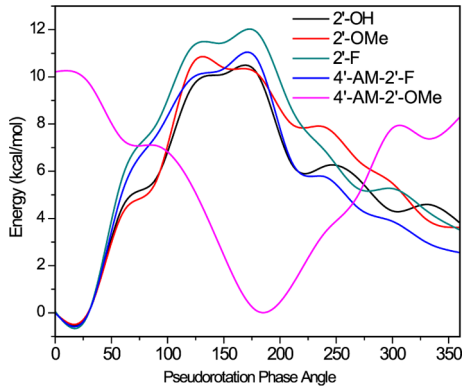

Figure 2. Pseudorotational phase angle (P) energy profile of modified and unmodified uridines. Energy values are from DFT calculations performed at PBE functional using 6-311++G* basis set in solvent (water).

conformers with P in the range of 169−180°, which corresponds to C2′-endo sugar pucker found in B-type DNA.[30,33] The same trend is observed for all modifications in the gas-phase calculations as well (Figure S3A, Supporting Information). In addition, DFT calculations in the gas phase were carried out on three reference nucleotides: 2′-deoxy-2′-S-methyluridine (2′-SMe),[34] 4′-AM-2′-deoxyuridine, and 4′-AM-uridine. Results indicate that 2′-SMe-uridine and 4′-AM-2′-deoxyuridine adopt a C2′-endo sugar conformation (Figure S4, Supporting Information). A similar conformational preference has been reported for 2′-deoxy-2′-(trifluoroethyl)uridine (2′-SCF_3), a bulky 2′modification that destabilizes the RNA duplex due to the unfavorable steric interaction with the 3′-neighboring nucleotide.[35] Interestingly, 4′-AM-uridine mainly prefers the C3′-endo conformation; however, this modification is flexible enough to adopt the C2′-endo sugar conformation as well (Figure S4, Supporting Information)

Scheme 1. Synthesis of 4′-AM-2′-F-uridine Nucleoside 8[a]

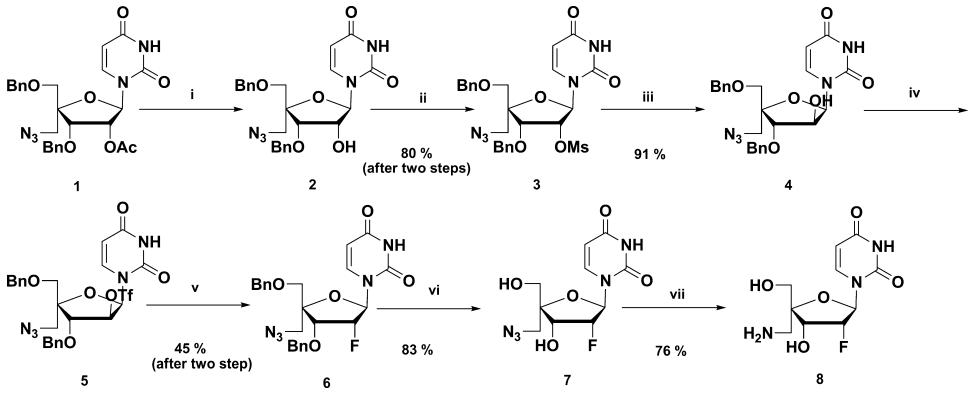

[a]Reagents and conditions: (i) NaOMe, MeOH, rt, 2 h; (ii) MsCl, pyridine, 0 °C, 6 h; (iii) 1 M NaOH, EtOH−H_2O (2:1, v/v), rt, 2 h; (iv) Tf_2O, DCM-pyridine (9:1, v/v), 0 °C, 2 h; (v) $Et_3N{\cdot}3HF$, Et_3N, toluene, 45 °C, 60 h; (vi) BCl_3, DCM, −78 °C, 3 h, then −30 °C, 3 h; (vii) PPh_3, H_2O, THF, 45 °C, 4 h.

dx.doi.org/10.1021/jo4012333 | J. Org. Chem. 2013, 78, 9956−9962

In 4′-AM-2′-F, sugar contains two additional torsion angles such as C2′−C3′−C4′−C (Ω) and O3′−C3′−C4′−C (ω), which adopt values of ∼72° and ∼−51°, respectively. The two additional torsion angles Ω and ω in 4′-AM-2′-OMe adopt values entirely different than that of 4′-AM-2′-F, which are ∼170° and ∼51°, respectively. The torsion angles in the sugar backbone γ(O5′−C5′−C4′−C3′) and δ(C5′−C4′−C3′−O3′) in 4′-AM-2′-F were able to adopt angles (∼52° and ∼86°) similar to those of native RNA (Table S1, Supporting Information).[22] However, γ and δ of 4′-AM-2′-OMe adopt values ∼35° and ∼110°, respectively, which is similar to those of native DNA (Table S1, Supporting Information).[22]

To probe potential H-bonding interactions in the sugar moiety, the distance between the hydrogen atom of CH_2 in the 4′-C-aminomethyl group and the F atom at the C2′ position has been measured from the conformations generated during the potential energy scan. For the lowest energy C3′-endo conformer, the distance between hydrogen and fluorine is found to be 2.3−2.5 Å with a C−H−F angle of 123−155°, which indicates the presence of a weak C−H···F H-bonding interaction (Figure 3).[36] The C−H···F H-bond was validated

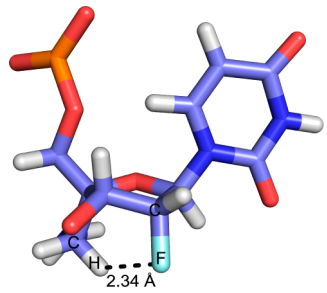

Figure 3. Low energy conformer of 4′-AM-2′-F-U from the potential energy scan utilizing PBE functional using 6-311++G* basis set in solvent. C3′-endo conformation in which C−H···F hydrogen bonding shown with dotted lines.

using noncovalent interactions (NCI) plot,[37] which showed the isosurface electron density between fluorine and hydrogen (Figure S5, Supporting Information). It should be noted that[38] C−H···F hydrogen bonds in 2′-FANA at the pyrimidine−purine steps are shown to increase the duplex affinity of modified oligonucleotides.[17] The combined strength of H-bond along with the gauche effect of the F2′−C2′−C1′−O4′ torsion stabilize 4′-AM-2′-F-U in C3′-endo by reducing the conformational flexibility of endocyclic torsions (Tables S1 and S2, Supporting Information).[30]

To compare the conformational dynamics of modifications, MD simulations (AMBER 12)[39] in explicit solvent were carried out with the same model system used in DFT calculations (Figure S2, Supporting Information). MD simulations started with 14 different sugar conformations of both modified and unmodified nucleotides.[40] Sugar torsions and conformations showed a similar trend, which was observed in the DFT calculations (Figure S3B, Supporting Information). RMSDs of all modifications showed maximum deviation up to 2.5 Å (Figure S6, Supporting Information).

The distributions of sugar puckering were calculated using their endocyclic torsional angle from the MD simulation trajectories and are plotted against *P* for every 5 ps. From these analyses it became evident that, as expected, 2′-OH, 2′-OMe, and 2′-F preferred the C3′-endo sugar conformation (Figure S7, Supporting Information). The 4′-AM-2′-F-U favored the C3′-endo sugar conformation along with 23% of C4′-exo pucker. The C−H···F H-bond observed in the 4′-AM-2′-F modification from the DFT calculations was retained during the course of MD simulations with H-bond occupancy of 96%. As revealed from DFT studies, 4′-AM-2′-OMe favored the C2′-endo pucker along with ∼5% of the population distributed in C3′-exo (Figure S7, Supporting Information).

The distribution of backbone torsions (α to ζ) for the 2′-OMe, 2′-F, and 4′-AM-2′-F did not show any substantial differences from those of a C3′-endo pucker (Table S3 and Figures S8−S10, Supporting Information). However, 4′-AM-2′-OMe-U deviates significantly in the γ, δ, ε, and ζ angles from that of the C3′-endo sugar pucker (Figures S9 and S10, Supporting Information). This deviation is due to the flexibility of the 4′-C-aminomethyl group evident from their two additional flexible torsional angles Ω (∼166° ± 33°) and ω (∼57° ± 40°),whereas in 4′-AM-2′-F Ω (∼75° ± 11°) and ω (∼−56° ± 13°) torsions were less fluctuating due to the presence of the C−H···F H-bond.

Sugar conformations determine the base-pairing geometry.[41] Here, to probe the H-bonding interactions, RNA duplex model systems (5′-GUC-3′/3′-CAG-5′) in which the middle uridine was replaced with modified nucleotides were utilized. To predict appropriate W−C H-bond distance and free energy of formation (PMF) between the bases, umbrella sampling simulations were exploited.[42] Free energy variation as a function of H-bond distance is represented in Figure 4. Each of the curves showed the global minimum (m_1) where the distance between the two bases adopt its most stable conformation.

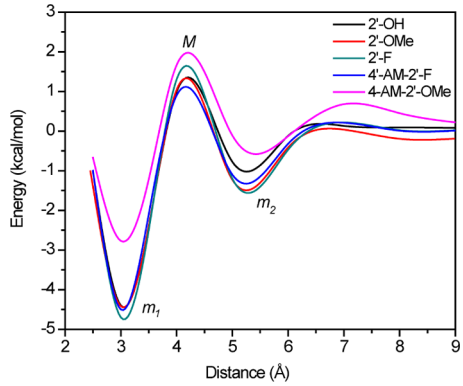

Figure 4. Free energy variations as a function of H-bond distance between nitrogenous bases. The free energy formation of the H-bond is calculated using 35 ns umbrella sampling simulations for each modification. Here, m_1, m_2 are the global minimum and local minimum, respectively, and *M* corresponds to the energy maximum.

Structures at the m_1 for all of the modifications are shown in Figure 5 and Figure S11 (Supporting Information). At the local minimum m_2, W−C H-bonding atoms in bases were bridged by a water molecule, and distances between two bases are ∼5.7 Å. The 2′-F-U-A pair was found to be most stable with a standard free energy of ΔG° −4.83 kcal/mol at a H-bond distance of 2.89 Å. This is in agreement with the reports that C2′-F nucleotides have higher H-bonding strength and stacking interactions compared to unmodified nucleotides.[43] Nucleotide pairs with next lowest energy are 2′-OH-U-A, 2′-OMe-U-A, and 4′-AM-2′-F-U-A at a H-bond distance of ∼2.9 Å (Figure S11, Supporting Information). The C1′−C1′ distances of 2′-

dx.doi.org/10.1021/jo4012333 | J. Org. Chem. 2013, 78, 9956−9962

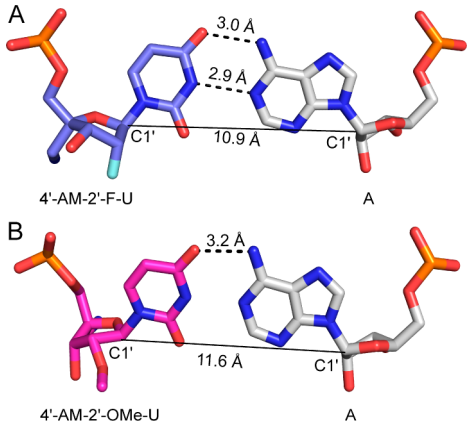

Figure 5. MD snapshot at m_1 of modified base pairs from the 35 ns of umbrella sampling simulations. The sugar conformations of (A) 4′-AM-2′-F and (B) 4′-AM-2′-OMe are represented with base pairing adenosine. Black dotted line represents the H-bond and their distances between the nitrogenous bases are shown in Å. The solid line represents the distance between C1′−C1′ of the U−A base pair.

OMe and 4′-AM-2′-F-U were found to be ∼10.9 Å. The 4′-AM-2′-OMe-U modification has larger C1′−C1′ distance of 11.6 Å, with a nonplanar base-pair geometry. Thus, this modification from only one H-bond (C−O···H−N) with base pair stabilization of −2.6 kcal/mol at 3.2 Å distance.[20]

It is known that hydration of bases is important for the stabilization of H-bonding between the bases.[44] At m_1, for the unmodified system, the W−C base pair was hydrated by five water molecules, of which three are present in the major groove and two in the minor groove position (Figure S12, Supporting Information). Similarly, 2′-F, 2-OMe, and 4′-AM-2′-F-U were hydrated by five water molecules. But 4′-AM-2′-OMe-U lost hydration completely in the minor groove. This loss in hydration attributes to the unstabilized base pairs and absence of a water mediated hydrogen bond at m_2.

The frequency distribution of χ angle (O4′−C1′−N1−C6) shows that 4′-AM-2′-F-U adopts a value of 169.5°, which is similar to that of unmodified (163.4°), 2′-OMe (160.7°), and 2′-F (165.7°) modifications (Figure S13, Supporting Information). Deviating from native C3′-endo conformation, 4′-AM-2′-OMe-U adopts C2′-endo like χ of 118.9°.[20] The deviation of χ disrupts the base pair geometry, and due to this 4′-AM-2′-OMe-U-A pair lost one H-bond, which was observed during umbrella sampling simulations (Figure 5).

In summary, we have carried out the synthesis of 4′-AM-2′-F-U with reasonable yields. From the NMR analysis it was evident that modified nucleoside adopts C3′-endo conformation in solution. DFT calculations and MD simulations using nucleotide model systems revealed that in 4′-AM-2′-F-U, a stronger gauche effect and C−H···F H-bond stabilizes C3′-endo sugar conformation, which results in normal W−C base pair formation. In contrast, 4′-AM-2′-OMe modification prefers C2′-endo sugar conformation and loses one W−C H-bond between the bases. These results also highlight the importance of 2′-substiutent in dictating conformational preference of 4′-*C*-aminomethyl nucleotides. Because of its C3′-endo conformational preference, 4′-AM-2′-F modification may find application in therapeutically appealing nucleic acids.

EXPERIMENTAL SECTION

General Methods. All chemicals and dry solvents (THF, MeOH) were obtained from commercial sources and used without any further purification. Acetonitrile, DCM, Et_3N, and pyridine were dried using calcium hydride. Toluene was dried using calcium chloride. Thin-layer chromatography (TLC) was performed on silica gel plates precoated with fluorescent indicator with visualization by UV light or by dipping into a solution of 5% concd H_2SO_4 in ethanol (v/v) and heating. Silica gel (100−200 mesh) was used for column chromatography. ^{1}H NMR (400 or 300 MHz), ^{13}C NMR (100 MHz), and ^{19}F NMR (376.5 MHz) were recorded on a 400 or 300 MHz instrument. The chemical shifts in parts per million (δ) are reported downfield from TMS (0 ppm) and referenced to the TMS signal or residual proton signal of the deuterated solvent as follows: TMS (0 ppm) or CD_3OD (3.31 ppm) for ^{1}H NMR spectra, and $CDCl_3$ (77.2 ppm) or CD_3OD (49.1 ppm) for ^{13}C NMR spectra. Multiplicities of ^{1}H NMR spin couplings are reported as s for singlet, bs for broad singlet, d for doublet, dt for doublet of triplets, dd for doublet of doublets, ddd for doublet of doublet of doublets, ABq for AB quartet, AXq for AX quartet, or m for multiplet and overlapping spin systems. Values for apparent coupling constants (J) are reported in Hz. High-resolution mass spectra (HRMS) were obtained in positive-ion electrospray ionization (ESI) mode using a Q-TOF analyzer.

4′-*C*-Azidomethyl-3′,5′-di-*O*-benzyl-2′-*O*-methanesulfonyluridine (3). Nucleoside **1** (0.2 g, 0.38 mmol) was dissolved in dry methanol (2 mL). To this 1 M sodium methoxide in methanol (0.6 mL) was added and the mixture stirred at room temperature for 2 h. Solvent was partially evaporated under reduced pressure and extracted with DCM (2 × 30 mL). The combined organic layer was dried over anhydrous Na_2SO_4, evaporated, co-evaporated with dry pyridine (2 × 20 mL), and dissolved in 2 mL of the same solvent. The reaction mixture was cooled in an ice bath, and methanesulfonyl chloride (0.06 mL, 0.77 mmol) was added dropwise and stirred at 4 °C for 6 h. The reaction was quenched with saturated aqueous $NaHCO_3$ (20 mL) and extracted with DCM (2 × 30 mL). The organic phase was dried over anhydrous Na_2SO_4, evaporated under reduced pressure, and coevaporated with toluene (2 × 20 mL) and DCM (2 × 20 mL). The crude compound was purified by column chromatography (40% ethyl acetate in hexane) to give **3** as a white solid (183 mg, 80%): R_f = 0.72 (20% ethyl acetate in petroleum ether): mp 75−76 °C; ^{1}H NMR (400 MHz, $CDCl_3$) δ: 9.77 (s, 1H), 7.77 (d, J = 7.9 Hz, 1H), 7.39−7.32 (m, 7H), 7.22−7.20 (m, 2H), 6.09 (d, J = 3.4, 1H), 5.27−5.22 (m, 2H), 4.86, 4.48 (AXq, J = 11.6 Hz, 2H), 4.43, 4.36 (ABq, J = 10.7, 2H), 4.36 (d, J = 6.04 Hz, 1H), 3.87, 3.47 (AXq, J = 10.6 Hz, 2H), 3.76, 3.35 (AXq, J = 13.6 Hz, 2H), 3.18 (s, 3H); ^{13}C NMR (100 MHz, $CDCl_3$) δ 162.9, 150.5, 139.8, 136.8, 128.8, 128.7, 128.6, 128.4, 128.2, 102.7, 88.1, 87.8, 79.7, 76.3, 74.2, 74.0, 70.8, 52.9, 39.0. HRMS (ESI) calcd for $C_{25}H_{28}N_5O_8S$ $[M + H]^+$ 558.1659, found $[M + H]^+$ 558.1678 (Δm +0.002, error, +3.6 ppm).

4′-*C*-Azidomethyl-3′,5′-di-*O*-benzylarabinouridine (4). Compound **3** (1.45 g, 2.59 mmol) was dissolved in ethanol−H_2O (2:1, v/v, 36 mL). To this was added 1 M NaOH (5.5 mL), and the reaction mixture was stirred at room temperature for 2 h. The reaction was neutralized with 6 M HCl (4−6 drops) and extracted with EtOAc (3 × 80 mL). The organic phase was dried over anhydrous Na_2SO_4 and evaporated under reduced pressure. The compound was purified by column chromatography (40% ethyl acetate in hexane) to afford nucleoside **4** as white solid (1.13 g, 91%): R_f = 0.42 (70% ethyl acetate in petroleum ether); mp 90−91 °C; ^{1}H NMR (400 MHz, $CDCl_3$) δ 10.6 (bs, 1H), 7.61 (d, J = 8 Hz, 1H), 7.37−7.25 (m, 10H), 6.23 (d, J = 3.8 Hz, 1H), 5.29 (d, J = 8.2 Hz, 1H), 5.01 (bs, 1H), 4.77, 4.55 (AXq, J = 11.3 Hz, 2H), 4.76 (d, J = 4.2 Hz, 1H), 4.52, 4.48 (ABq, J = 11.3 Hz, 2H), 4.16 (d, J = 2.2 Hz, 1H), 3.64, 3.45 (AXq, J = 12.6 Hz, 2H), 3.69, 3.66 (ABq, J = 9.6 Hz, 2H); ^{13}C NMR (100 MHz, $CDCl_3$) δ 165.6, 150.7, 142.9, 137.5, 137.4, 128.7, 128.6, 128.2, 128.1, 128.1, 100.7, 86.6, 86.1, 83.8, 74.3, 73.8, 72.5, 70.0, 52.2; HRMS (ESI) calcd for $C_{24}H_{26}N_5O_6$ $[M + H]^+$ 480.1883, found $[M + H]^+$ 480.1882 (Δm −0.0001, error, −0.2 ppm).

4′-*C*-Azidomethyl-3′,5′-di-*O*-benzyl-2′-deoxy-2′-fluorouridine (6). Compound **4** (200 mg, 0.42 mmol) was dissolved in DCM/

dx.doi.org/10.1021/jo4012333 | J. Org. Chem. 2013, 78, 9956−9962

pyridine (3:1, v/v, 4 mL) and stirred in an ice bath. Tf_2O (0.08 mL, 0.50 mmol) was added dropwise under nitrogen atmosphere and the mixture stirred for 2 h. The reaction was quenched with cold saturated aqueous $NaHCO_3$ (50 mL) and extracted with DCM (3 × 80 mL). The organic phase was dried over anhydrous Na_2SO_4, evaporated under reduced pressure followed by co-evaporation with toluene (2 × 30 mL), and dried. The crude compound **5** was dissolved in dry toluene (10 mL). $Et_3N{\cdot}3HF$ (0.07 mL, 1.67 mmol) and Et_3N (0.12 mL, 0.83 mmol) were added and the mixture heated at 45 °C. After 12 h, an additional batch of $Et_3N{\cdot}3HF$ (0.14 mL, 0.83 mmol) and Et_3N (0.12 mL, 0.83 mmol) were added, and the reaction mixture was heated for 48 h. Toluene was evaporated under reduced pressure, and the residue was dissolved in ethyl acetate (70 mL) and washed with satd $NaHCO_3$ (40 mL). The aqueous layer was extracted with ethyl acetate (3 × 70 mL). The organic phase was dried over anhydrous Na_2SO_4 and evaporated under reduced pressure. The crude compound was purified by column chromatography (25% ethyl acetate in hexane) to give compound **6** as yellow sticky solid (90 mg, 45%): R_f = 0.52 (40% ethyl acetate in petroleum ether); ^{1}H NMR (300 MHz, $CDCl_3$) δ 9.25 (bs, 1H), 7.69 (d, J = 8.1 Hz, 1H), 7.36−7.22 (m, 11 H), 6.2 (dd, J = 15.5 Hz, 2.6 Hz, 1H), 5.3 (d, J = 8.1 Hz, 1H), 5.10 (ddd, J = 53 Hz, 5.2 Hz, 2.87 Hz, 1H), 4.80, 4.52 (AXq, J = 11.6 Hz, 2H), 4.50, 4.46 (ABq, J = 11.6 Hz, 2H), 4.33 (dd, J = 16.7 Hz, 4.6 Hz, 1H), 3.87, 3.56 (AXq, J = 10.4 Hz, 2H), 3.71, 3.42 (AXq, J = 13.5 Hz, 2H); ^{13}C NMR (100 MHz, $CDCl_3$) δ 163.3, 150.2, 140.3, 136.9, 128.8, 128.7, 128.6, 128.5, 128.3, 128.2, 102.5, 92.5 (d, J = 194.5, 1C), 88.3 (d, J = 33.2 Hz, 1C), 87.5, 76.5 (d, J = 14.2 Hz, 1C), 74.0, 73.6, 70.8, 52.9; ^{19}F NMR (376.5 MHz, $CDCl_3$) δ −199.1 (dt, J = 52.8 Hz, 17.3 Hz, 1F); HRMS (ESI) calcd for $C_{24}H_{25}N_5O_5F$ $[M + H]^+$ 482.1840, found $[M + H]^+$ 482.1832 (Δm −0.0008, error, −1.7 ppm).

4′-*C*-Azidomethyl-2′-deoxy-2′-fluorouridine (7). Nucleoside **6** (50 mg, 0.103 mmol) was dissolved in DCM (2 mL). The solution was cooled to −78 °C, BCl_3 (0.7 mL, 1 M solution in DCM) was added, and the mixture was stirred at −78 °C for 3 h. The temperature was increased to −30 °C and the mixture stirred again for 3 h. The reaction mixture was quenched using a 1:1 mixture of DCM−MeOH (v/v, 1 mL). Solvent was evaporated and purified using column chromatography (5% methanol in DCM) to afford compound **7** as a white sticky solid (25 mg, 83%): R_f = 0.3 (5% methanol in DCM); ^{1}H NMR (400 MHz, CD_3OD) δ 8.01 (d, J = 8.0 Hz, 1H), 6.2 (dd, J = 14.8 Hz, 4.5 Hz, 1H), 5.72 (d, J = 8 Hz, 1H), 5.22 (dt, J = 53.5 Hz, 4.6 Hz, 1H), 4.51 (dd, J = 12.2 Hz, 5 Hz, 1H), 3.78, 3.68 (ABq, J = 11.7 Hz, 2 H), 3.60, 3.44 (ABq, J = 13.2 Hz, 2H); ^{13}C NMR (100 MHz, CD_3OD) δ 166.2, 152.3, 142.8, 103.2, 95 (d, J = 190.5 Hz, 1C), 89.7, 88.7 (d, J = 33.1 Hz, 1C), 71.3 (d, J = 15.4 Hz, 1C), 64.2, 53.3; ^{19}F NMR (376.5 MHz, CD_3OD) δ −205.2 (dt, J = 52.1 Hz, 13.9 Hz, 1F); HRMS (ESI) calcd for $C_{10}H_{13}N_5O_5F$ $[M + H]^+$ 302.0901, found $[M + H]^+$ 302.0887 (Δm −0.0013, error, −4.4 ppm).

4′-*C*-Aminomethyl-2′-deoxy-2′-fluorouridine (8). Nucleoside **7** (20 mg, 0.07 mmol) was dissolved in THF (1.5 mL). To this, water (0.05 mL) and PPh_3 (34 mg, 0.132 mmol) were added. The reaction mixture was stirred at 45 °C for 3 h. Solvent was evaporated and and the mixture purified by preparative TLC (80% ethyl acetate in petroleum ether) to give fluoro nucleoside **8** as a pale yellow solid (14 mg, 76%): R_f = 0.15 (40% MeOH in DCM); mp 160−161 °C; ^{1}H NMR (400 MHz, CD_3OD) δ 7.98 (d, J = 8.0 Hz, 1H), 6.2 (dd, J = 14.8 Hz, 4.8 Hz, 1H), 5.72 (d, J = 8 Hz, 1H), 5.22 (dt, J = 53.4 Hz, 5.0 Hz, 1H), 4.51 (dd, J = 11.1 Hz, 5.3 Hz, 1H), 3.71, 3.68 (ABq, J = 11.9 Hz, 2 H), 2.99, 2.84 (ABq, J = 13.7 Hz, 2H); ^{13}C NMR (100 MHz, CD_3OD) δ 166.8, 152.8, 143.0, 103.2, 95 (d, J = 191.2 Hz, 1C), 89.2, 89 (d, J = 33.6 Hz, 1C), 72.5 (d, J = 15.4 Hz, 1C), 65.3, 42.3. ^{19}F NMR (376.5 MHz, CD_3OD) δ −205.6 (dt, J = 54.8 Hz, 12.9 Hz, 1F); HRMS (ESI) calcd for $C_{10}H_{15}N_3O_5F$ $[M + H]^+$ 276.0996, found $[M + H]^+$ 276.0986 (Δm −0.001, error, −3.6 ppm).

Sugar Conformational Analysis Using PSEUROT Program. The coupling constant (J) derived from ^{1}H NMR of the free nucleoside in methanol-d_4 was used for the sugar conformational analysis with PSEUROT program.[29] Using the electronegativity editor in the program, the nature of the substituent such as fluorine at C2′ and aminomethyl at C4′ of the five-membered ring was assigned. The scanning was performed with ν_{max} and started from 10° to 60° and P from 0° to 360°; a total of 3600 grid points were scanned to find the minimum energy surface of the nucleoside in P. The temperature was set to 22 °C, which was used for recording NMR; all other parameters were retained as default in the program.[29]

Sugar Conformational Analysis Using DFT Calculations. The model used in this study contains modified nucleosides in the middle and is capped with sugar phosphate at the 3′ and 5′ end (Figure S1, Supporting Information). To avoid the complexity from stacking interactions between the bases, bases were removed from both ends of the sugar and replaced with methyl groups. The sugar conformation at both ends was frozen to the C3′-endo conformer, and the potential energy for the sugar conformations of the modified nucleotides were calculated using DFT level (MP2/6-311++G*) in Gaussian 09.[45] For each modification, different sugar−phosphate dihedrals were chosen from the Nucleic Acid Database (NDB),[40] and calculations were performed in the gas phase and in implicit solvent. A potential energy scan was performed around the pseudorotation phase angle (P) with increments of 0.5° yielding 720 conformations for each modification. For each of these conformations, initially the structures were first optimized in the HF/6-31G* level, and then energies were obtained at MP2/6-311++G* level.[31] To investigate the effect of solvent (water) on the sugar conformation, the structures were initially optimized at HF/6-31G* level, and energies were obtained at the PBE density functional, 6-311++G* basis set.[30] For solvation in DFT calculations the PCM model was used.[46]

C−H···F H-Bond Analysis Using NCI Plot. A low energy conformer obtained from DFT calculations in the solvent phase of 4′-AM-2′-F-uridine was used for plotting reduced density gradient(s) against electron density (ρ).[37] To identify only the hydrogen bonds and electrostatic interactions, excluding the van der Waals interactions, the ρ value was set from 0.02−0.06 au. The output from the NCI program was plotted using gnuplot, and the H-bond surface was rendered using VMD 1.9.1.

Sugar Conformational Analysis Using MD Simulations. The same model system used for the DFT calculations was employed for the MD simulations using AMBER 12.[39] Modified nucleotides 2′-F and 4′-AM-2′-F uridine were optimized using Gaussian 09 at the HF/6-31G* level, and the force field was obtained using the protocol published by Aduri and co-workers[47] (Figures S14 and S15, Supporting Information). Initial coordinates for the model system were chosen from the 14 different sugar conformers with different P values, which are obtained from NDB.[40] For each sugar conformation, 5 ns of production run were carried out yielding 70 ns (14 × 5 = 70) simulations for each modification. Using van der Waals and 1−4 electrostatic interactions, the energy of the system at each sugar conformation was calculated from every 5 ns of the total 70 ns MD simulations. In all simulations, the AMBER force field with revised torsional parameters χ and α/γ was used,[48] and charges of the systems were neutralized using Na^+ ions. A TIP3P water box was used to solvate the system around 6 Å from any atom of the solute. Structures were minimized in three steps: (i) by fixing the model system, solvent and ions were minimized using steepest descent of 2500 steps; (ii) while the modified nucleotide was detained with a restraint force of 500 kcal/mol Å^2, steepest descent minimization of 5000 steps was followed by 5000 steps of conjugate gradient minimization: and (iii) without any restraints, steepest descent minimization of 1000 steps was followed by 1000 steps of conjugate gradient minimization. After the minimization, pressure equilibration were carried out in two steps, in which the modified nucleotide was fixed with a restraint force 25 kcal/mol Å^2 and a long-range cutoff of 8 Å. SHAKE was used for bonds involving hydrogen atoms. The temperature was raised from 0 to 300 K. In the second step, all of the above conditions were maintained except the temperature was kept constant and pressure dynamics was used. Minimization and equilibration were carried out using the SANDER module, and production runs were carried out with the PMEMD in AMBER 12.[39]

H-Bonding Analysis Using Umbrella Sampling Simulations. Trinucleotide RNA duplex (5′-GUC-3′/3′-CAG-5′) was generated using the *nucgen* module in AMBER12.[39] Uridine was replaced with

dx.doi.org/10.1021/jo4012333 | J. Org. Chem. 2013, 78, 9956−9962

modified nucleotides such as 2′-OMe, 2′-F, 4′-AM-2′-F, and 4′-AM-2′-OMe. The AMBER force field with revised torsional parameters for χ and α/γ was used.[48] The system was initially minimized at vacuum to reach low energy geometries and further used for the restraint angle determination. All of five trinucleotide systems with different modifications, including an unmodified system, were solvated in an octahedral box using TIP3P water and neutralized with and Na^+ ions.[49] The SHAKE algorithm was used to constrain the bonds involving hydrogen atoms. Solvated systems were initially minimized in two steps; at first the positional restraints were applied to the nucleotides to minimize the solvent and ions. Finally, unrestrained minimizations were applied to the whole solvated system. Various sampling times were performed for each system to predict the error in the final energy calculation (Tables S4−S8, Supporting Information), and the free energy errors were within the acceptable limit[41] (Table S9, Supporting Information). All of the parameters for performing the final equilibrations and MD simulations were obtained from the published protocol.[41] The reaction co-ordinates were recorded every five steps, and the WHAM algorithm potential mean force was obtained as a function of H-bond distance with a tolerance of 0.00001.[50] Trajectories were visualized using UCSF Chimera, and the figures were rendered using PyMOL v0.99.

■ ASSOCIATED CONTENT

Ⓢ Supporting Information

Additional data from DFT calculations, MD simulations, and NMR spectra of all the new compounds. This material is available free of charge via the Internet at http://pubs.acs.org.

■ AUTHOR INFORMATION

Corresponding Author

*E-mail: pradeep@chem.iitb.ac.in.

Author Contributions

†K.R.G. and S.H. contributed equally to this work

Notes

The authors declare no competing financial interest.

■ ACKNOWLEDGMENTS

We are thankful to the Computer Centre, IIT Bombay, for providing high-performance computing facility and SAIF-IIT Bombay for NMR spectra. We are also thankful to Prof. David A. Case for waiving of the licensing fee for AMBER12, Prof. R. B. Sunoj and Mr. Bangaru Bhaskararao for helpful discussions regarding hydrogen bond analysis, and Prof. R. Murugavel for providing access to X-ray facility. This work is financially supported by grants from Department of Biotechnology (DBT)-Government of India (RNAi-Technologies Platform, BT/PR10693/AGR/36/586/2008) and IRCC-IIT Bombay. P.I.P is a recipient of Max Planck India Fellowship (MPG-DST Scheme). K.R.G. thanks the University Grants Commission (UGC) and S.H. thanks Department of Atomic Energy-Board of Research in Nuclear Sciences (DAE-BRNS), Government of India (Grant No. 2012/37C/4/BRNS-1063) for fellowships.

■ DEDICATION

Dedicated to Professor Krishna N. Ganesh on the occasion of his 60th birthday.

■ REFERENCES

(1) Bennett, C. F.; Swayze, E. E. *Annu. Rev. Pharmacol. Toxicol.* **2010**, *50*, 259−293.

(2) Keefe, A. D.; Pai, S.; Ellington, A. *Nat. Rev. Drug Discovery* **2010**, *9*, 537−550.

(3) Shukla, S.; Sumaria, C. S.; Pradeepkumar, P. I. *ChemMedChem.* **2010**, *5*, 328−349.

(4) Burnett, J. C.; Rossi, J. J. *Chem Biol.* **2012**, *19*, 60−71.

(5) Phelps, K.; Morris, A.; Beal, P. A. *ACS Chem. Biol.* **2012**, *7*, 100−109.

(6) Pallan, P. S.; Greene, E. M.; Jicman, P. A.; Pandey, R. K.; Manoharan, M.; Rozners, E.; Egli, M. *Nucleic Acids Res.* **2011**, *39*, 3482−3495.

(7) Manoharan, M.; Akinc, A.; Pandey, R. K.; Qin, J.; Hadwiger, P.; John, M.; Mills, K.; Charisse, K.; Maier, M. A.; Nechev, L.; Greene, E. M.; Pallen, P. S.; Rozners, E.; Rajeev, K. G.; Egli, M. *Angew. Chem., Int. Ed.* **2011**, *50*, 2284−2288.

(8) Deleavey, G. F.; Damha, M. J. *Chem. Biol.* **2012**, *19*, 937−954.

(9) Watts, J. K.; Choubdar, N.; Sadalapure, K.; Robert, F.; Wahba, A. S.; Pelletier, J.; Pinto, B. M.; Damha, M. J. *Nucleic Acids Res.* **2007**, *35*, 1441−1451.

(10) Pfundheller, H. M.; Wengel, J. *Bioorg. Med. Chem. Lett.* **1999**, *9*, 2667−2672.

(11) Pfundheller, H. M.; Bryld, T.; Olsen, C. E.; Wengel, J. *Helv. Chim. Acta* **2000**, *83*, 128−151.

(12) Manoharan, M. *Biochim. Biophys. Acta* **1999**, *1489*, 117−130.

(13) Lubini, P.; Zürcher, W.; Egli, M. *Chem. Biol.* **1994**, *1*, 39−45.

(14) Prakash, T. P.; Allerson, C. R.; Dande, P.; Vickers, T. A.; Sioufi, N.; Jarres, R.; Baker, B. F.; Swayze, E. E.; Griffey, R. H.; Bhat, B. *J. Med. Chem.* **2005**, *48*, 4247−4253.

(15) Teplova, M.; Minasov, G.; Tereshko, V.; Inamati, G. B.; Cook, P. D.; Manoharan, M.; Egli, M. *Nat. Struct. Biol.* **1999**, *6*, 535−539.

(16) Fauster, K.; Hartl, M.; Santner, T.; Aigner, M.; Kreutz, C.; Bister, K.; Ennifar, E.; Micura, R. *ACS Chem. Biol.* **2012**, *7*, 581−589.

(17) Anzahaee, M. Y.; Watts, J. K.; Alla, N. R.; Nicholson, A. W.; Damha, M. J. *J. Am. Chem. Soc.* **2011**, *133*, 728−731.

(18) Veedu, R. N.; Wengel, J. *Chem. Biodiversity* **2010**, *7*, 536−542.

(19) Srivastava, P.; Barman, J.; Pathmasiri, W.; Plashkevych, O.; Wenska, M.; Chattopadhyaya, J. *J. Am. Chem. Soc.* **2007**, *129*, 8362−8379.

(20) Gore, K. R.; Nawale, G. N.; Harikrishna, S.; Chittoor, V. G.; Pandey, S. K.; Höbartner, C.; Patankar, S.; Pradeepkumar, P. I. *J. Org. Chem.* **2012**, *77*, 3233−3245.

(21) Nawale, G. N.; Gore, K. R.; Höbartner, C.; Pradeepkumar, P. I. *Chem.Comm.* **2012**, *48*, 9619−9621.

(22) Saenger, W. *Principles of Nucleic Acid Structure*; Springer-Verlag: New York, 1984; ISBN: 03-8790-761-0.

(23) Varghese, O. P.; Barman, J.; Pathmasiri, W.; Plashkevych, O.; Honcharenko, D.; Chattopadhyaya, J. *J. Am. Chem. Soc.* **2006**, *128*, 15173−15187.

(24) Esmurziev, A.; Simic, N.; Sundby, E.; Hoff, B. H. *Carbohydr. Res.* **2010**, *29*, 348−367.

(25) Seela, F.; Chittepu, P. *Org. Biomol. Chem.* **2008**, *6*, 596−607.

(26) Takamatsu, S.; Maruyama, T.; Katayama, S.; Hirose, N.; Naito, M.; Izawa, K. *J. Org. Chem.* **2001**, *66*, 7469−7477.

(27) Honcharenko, D.; Varghese, O. P.; Plashkevych, O.; Barman, J.; Chattopadhyaya, J. *J. Org. Chem.* **2006**, *71*, 299−314.

(28) Jin, S.; Miduturu, C. V.; McKinney, D. C.; Silverman, S. K. *J. Org. Chem.* **2005**, *70*, 4284−4299.

(29) Hendrickx, P. M. S.; Martins, J. C. *Chem. Cent. J.* **2008**, *2*, 20−27.

(30) Thibaudeau, C.; Acharya, P.; Chattopadhyaya, J. *Stereoelectronic Effects in Nucleosides & Nucleotides and their Structural Implications*; Uppsala University Press: Uppsala, 1999; ISBN: 91-506-1351-0.

(31) Frisch, M. J.; Head-Gordon, M.; Pople, J. A. *Chem. Phys. Lett.* **1990**, *16*, 6281−289.

(32) (a) Perdew, J. P.; Burke, K. M.; Ernzerhof, M. *Phys. Rev. Lett.* **1997**, *78*, 1396−1396. (b) Perdew, J. P.; Burke, K.; Ernzerhof, M. *Phys. Rev. Lett.* **1996**, *77*, 3865−3868.

(33) Altona, C.; Sundaralingam, M. *J. Am. Chem. Soc.* **1972**, *94*, 8205−8212.

(34) Venkateswarlu, D.; Lind, K. E.; Mohan, V.; Manoharan, M.; Ferguson, D. M. *Nucleic Acids Res.* **1999**, *27*, 2189−2195.

(35) Fauster, K.; Kreutz, C.; Micura, R. *Angew. Chem., Int. Ed.* **2012**, *51*, 13080−13084.
(36) Egli, M. *Acc. Chem. Res.* **2012**, *45*, 1237−1246.
(37) Contreras-García, J.; Johnson, E. R.; Keinan, S.; Chaudret, R.; Piquemal, J.-P.; Beratan, D. N.; Yang, W. *J. Chem. Theory Comput.* **2011**, *7*, 625−632.
(38) Auffinger, P.; Westhof, E. *J. Mol. Biol.* **1997**, *274*, 54−63.
(39) Case, D. A. *AMBER 12*, University of California, San Francisco, 2012.
(40) Berman, H. M.; Olson, W. K.; Beveridge, D. L.; Westbrook, J.; Gelbin, A.; Demeny, T.; Hsieh, S. H.; Srinivasan, A. R.; Schneider, B. *Biophys. J.* **1992**, *63*, 751−759.
(41) Williams, A. A.; Darwanto, A.; Theruvathu, J. A.; Burdzy, A.; Neidigh, J. W.; Sowers, L. C. *Biochemistry* **2009**, *48*, 11994−12004.
(42) Stofer, E.; Chipot, C.; Lavery, R. *J. Am. Chem. Soc.* **1999**, *121*, 9503−9508.
(43) Patra, A.; Paolillo, M.; Charisse, K.; Manoharan, M.; Rozners, E.; Egli, M. *Angew. Chem., Int. Ed.* **2012**, *51*, 11863−11866.
(44) Sundaralingam, M.; Pan, B. C. *Biophys. Chem.* **2002**, *95*, 273−282.
(45) Gaussian 09, Revision A.02: Frisch, M. J. Gaussian, Inc., Wallingford, CT, 2009.
(46) Cossi, M.; Rega, N.; Scalmani, G.; Barone, V. *J. Comput. Chem.* **2003**, *24*, 669−681.
(47) Aduri, R.; Psciuk, B. T.; Saro, P.; Taniga, H.; Schlegel, H. B.; SantaLucia, J. *J. Chem. Theory Comput.* **2007**, *3*, 1464−1475.
(48) Cornell, W. D.; Cieplak, P.; Bayly, C. I.; Gould, I. R.; Merz, K. M.; Ferguson, D. M.; Spellmeyer, D. C.; Fox, T.; Caldwell, J. W.; Kollman, P. A. *J. Am. Chem. Soc.* **1995**, *117*, 5179−5197.
(49) Jorgensen, W. L.; Chandrasekhar, J.; Madura, J. D.; Impey, R. W.; Klein, M. L. *J. Chem. Phys.* **1983**, *79*, 926−935.
(50) Kumar, S.; Bouzida, D.; Swendsen, R. H.; Kollman, P. A.; Rosenberg, J. M. *J. Comput. Chem.* **1992**, *13*, 1011−1021.

Supporting Information

Influence of 2'-Fluoro versus 2'-*O*-Methyl Substituent on the Sugar Puckering of 4'-*C*-Aminomethyl-Uridine

Kiran R. Gore, Harikrishna, S. and Pradeepkumar, P.I.*
Department of Chemistry, Indian Institute of Technology Bombay,
Powai, Mumbai 400076, India
Email: pradeep@chem.iitb.ac.in

TABLE OF CONTENTS

Population distribution of 4'-AM-2'-F-uridine from PSEUROT

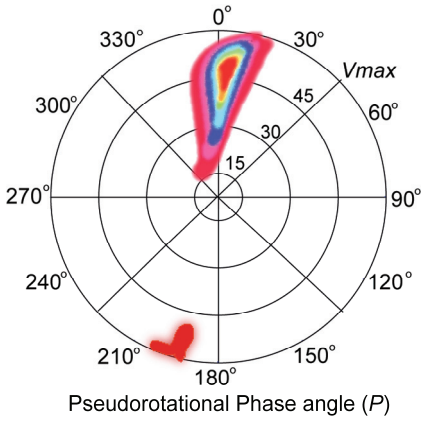

Figure S1. Population distribution of sugar conformation in 4'-AM-2'-F-uridine nucleoside. The five endocyclic torsion angles ν_0=44.863°, ν_1=37.583°, ν_2=5.948°, ν_3=11.779° and ν_4= −35.007° were obtained from the PSEUROT.[1] The RGB colours in the plot indicate the density of the population distribution from lower to higher. More than 90% of the sugar conformations are populated in C3'-endo sugar conformation. There are also few conformers found in the C2'-endo sugar conformation with *P* of 186°-200° and φ_m of 36°-52°. This results show that the conformation of the nucleoside is restricted at the nucleoside level itself in the solution phase.

Model system used for the DFT and MD simulation study

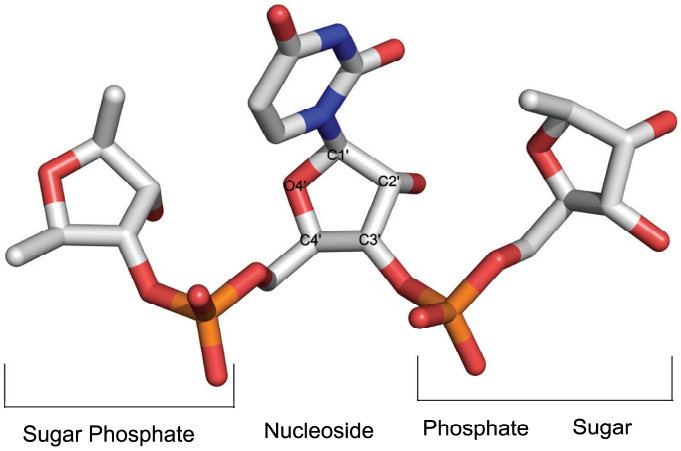

Figure S2. Model system used for the computational studies. Nucleoside at the middle in the model system is protected with sugar and phosphate groups at the 3'- and 5- ends. The 2'and 4'labeled sugar carbons are substituted with the corresponding modifications to perform potential energy scan using DFT calculations and MD simulations.

Pseudorotational phase angle energy profile from DFT and MD simulation

A B

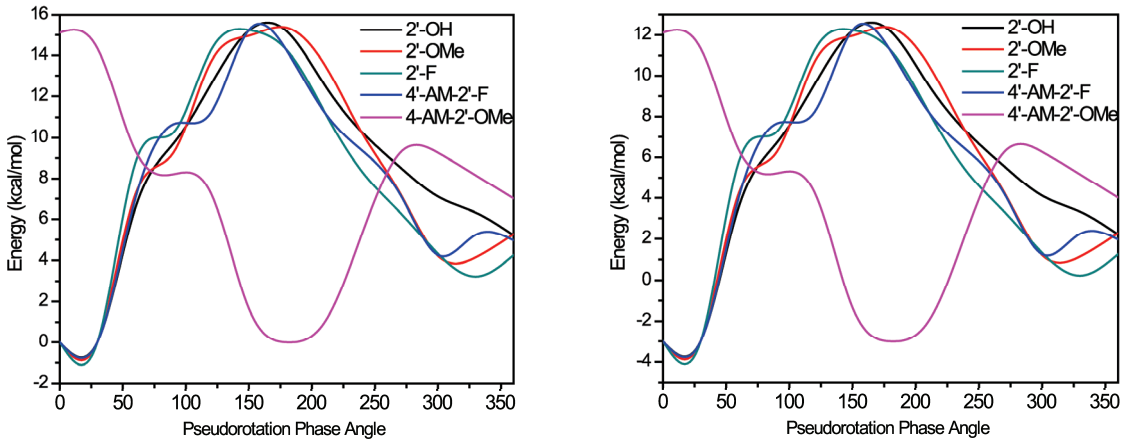

Figure S3. Energy versus pseudo rotational phase angle profiles from the DFT calculations in gas phase and molecular dynamics simulations for the modified and unmodified uridines: (A) using Gaussian 09 (MP2/6-311++G* level) and (B) using AMBER *force field*.

Pseudorotational phase angle energy profile from DFT in gas phase

A B

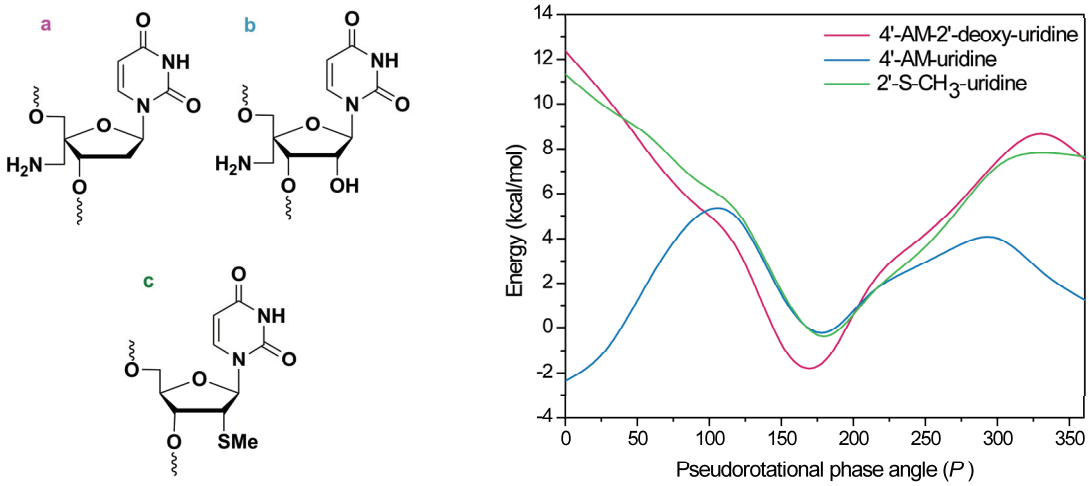

Figure S4. Energy versus pseudorotational phase angle profile of modified uridines from DFT calculations in gas phase. (A) Chemical structures of uridine employed for DFT calculations in tri-nucleotide model system (a) 4'-*C*-aminomethyl-2'-deoxy-uridine, (b) 4'-*C*-aminomethyl-uridine, (c) 2'-deoxy-2'-thiomethyl-uridine and (B) Energy profile of the modified uridine using Gaussian 09 (MP2/6-311++G* level).

Isosurface density plot for hydrogen bond in 4'-AM-2'-F-uridine

A

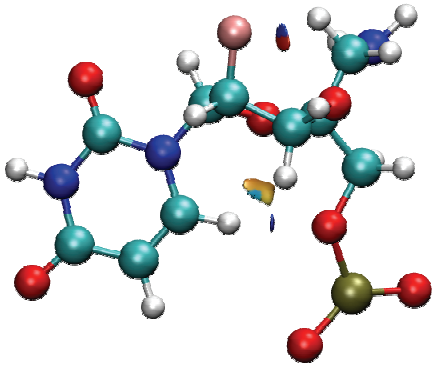

B

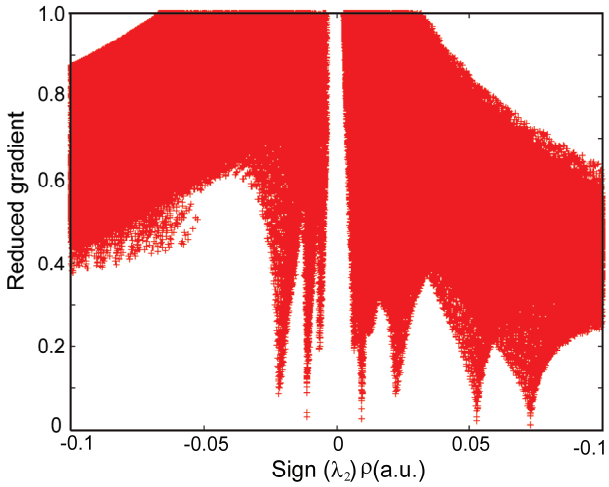

Figure S5. Intra-molecular isosurface and non-covalent interactions plot of 4'-AM-2'-F-uridine using Non-covalent interactions (NCI) plot.[2] (A) The isosurface plot shows the H-bond interactions between 2'-fluorine and hydrogen in 4'-*C*-aminomethyl group, and O4' in the sugar with the C6-H in the nucleobase. (B) Reduced gradient against electron density (ρ) plot for the self consistent field. Two peaks appeared between –0.05 to 0 indicates signify the presence of two weak H-bonds in 4'-AM-2'-F-uridine.

RMSD graphs of modified and unmodified nucleotides

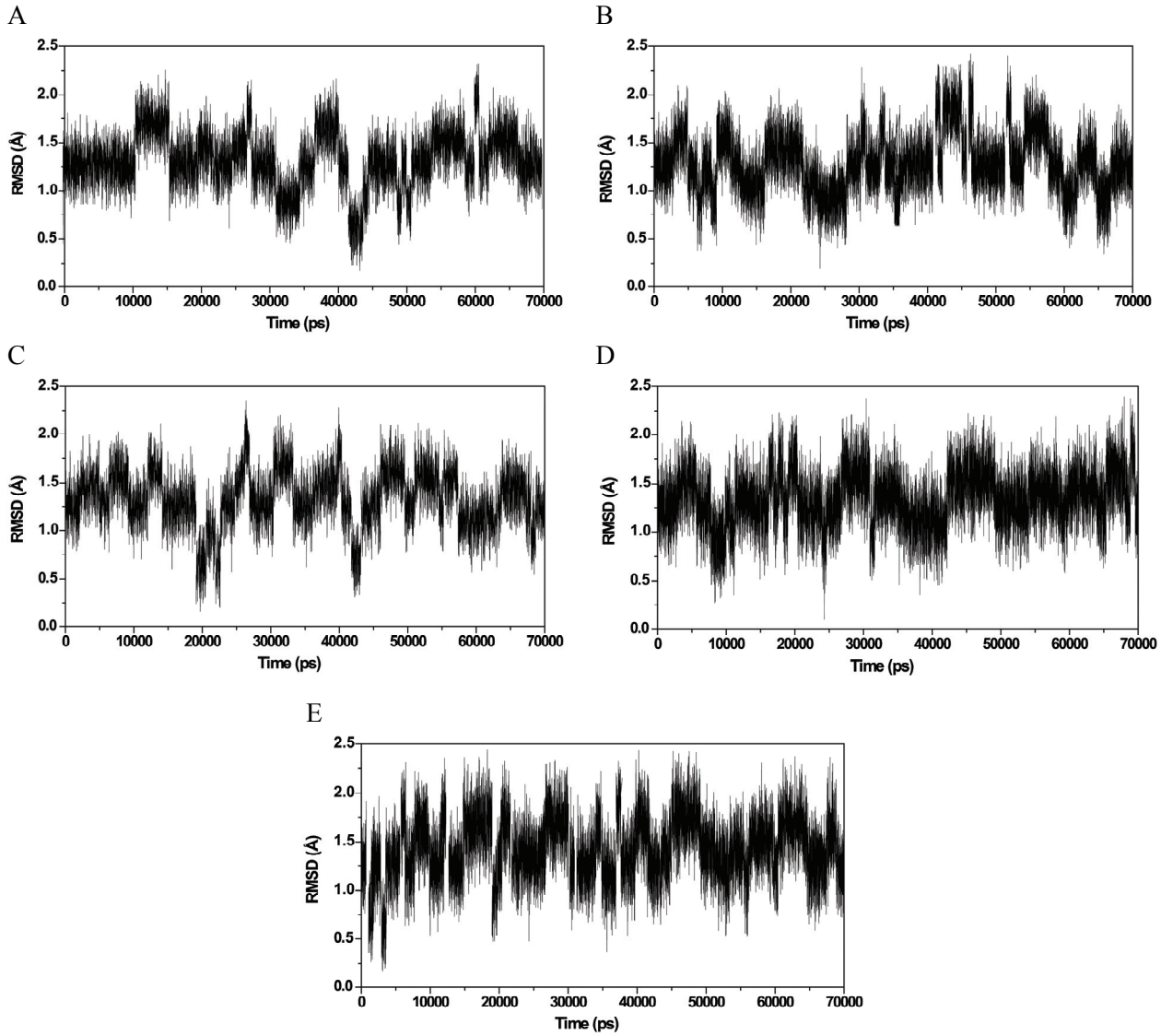

Figure S6. Root mean square deviation graphs of trajectories obtained from MD simulation of (A) 2'-OH, (B) 2'-OMe, (C) 2'-F, (D) 4'-AM-2'-F and (E) 4'-AM-2'-OMe uridine. RMSD values from the MD trajectories were calculated with the corresponding initial structure using ptraj module in AMBER 12.[3,4]

Pseudo rotational phase angle occupancy of modified and unmodified nucleotides

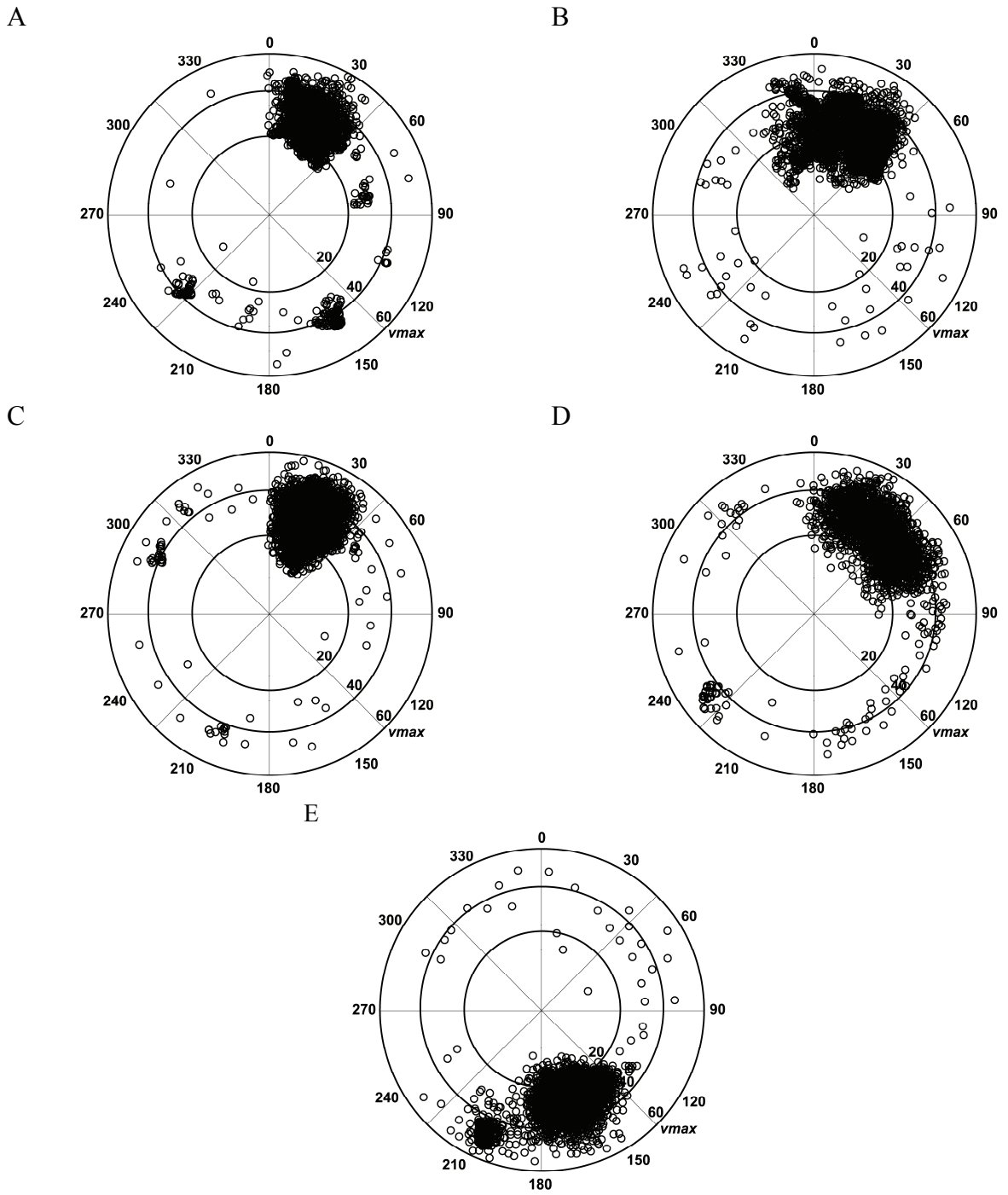

Figure S7. Pseudo rotational phase angle (*P*) occupancy over 70 ns of MD simulations of (A) 2'-OH, (B) 2'-OMe, (C) 2'-F, (D) 4'-AM-2'-F, and (E) 4'-AM-2'-OMe uridine. *P* values from the MD trajectories were calculated using ptraj module in AMBER 12. It was observed that 99.2% of the C3'-endo conformations of 4'-AM-2'-F found to have a weak C−H···F H-bond at 2.3 Å - 2.5 Å distance, which provide additional stabilization for the C3'-endo puckering.

Population density map of Alpha (α) and Beta (β) angle

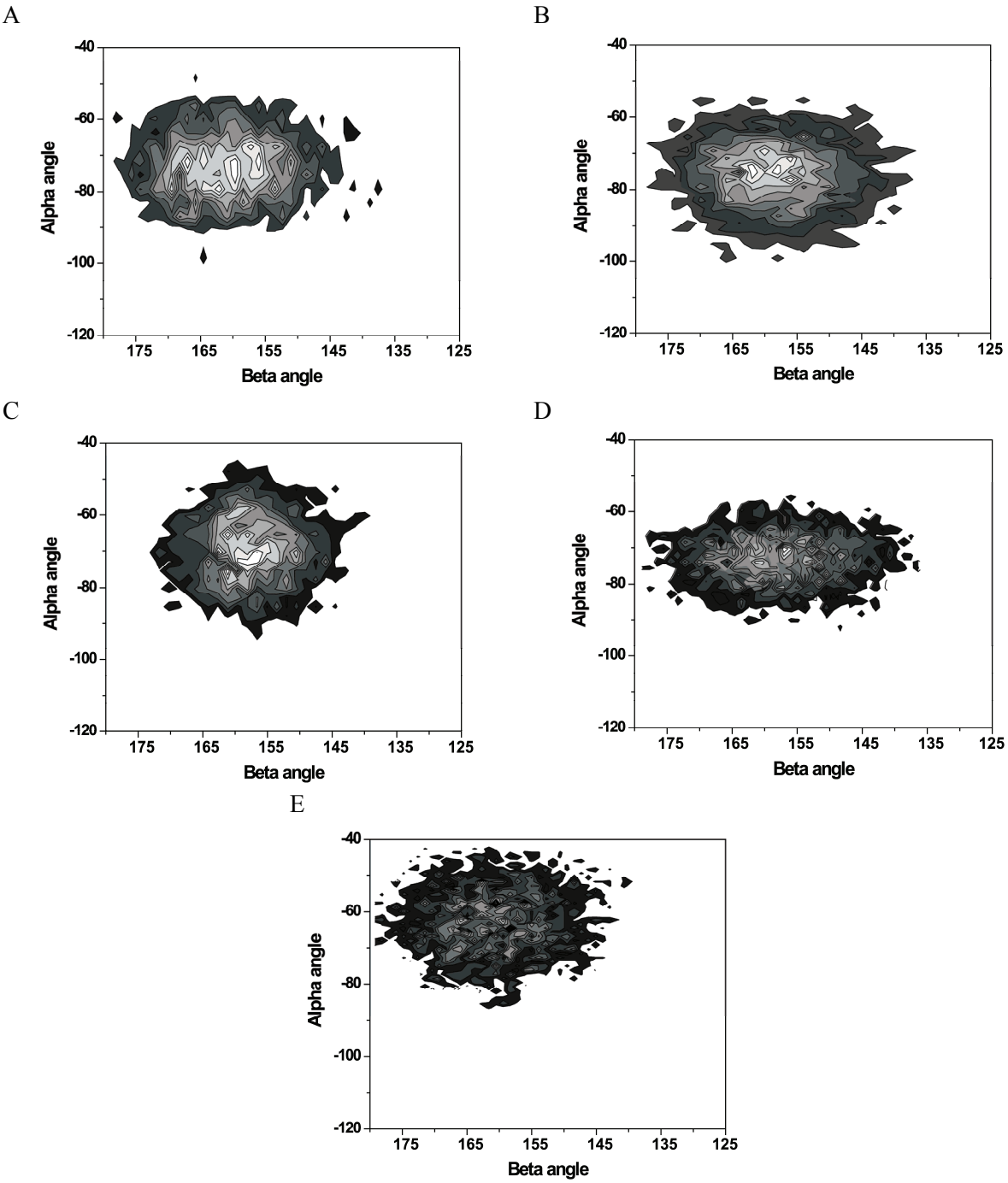

Figure S8. Population density map of the two dihedral angles the alpha and beta over the 70 ns of MD simulations: (A) 2'-OH, (B) 2'-OMe, (C) 2'-F, (D) 4'-AM-2'-F, and (E) 4'-AM-2'-OMe uridine. Increasing color contrasts from white to black indicate the decrease in the populations of sugar-phosphate dihedrals.[5]

Population density map of Gamma (γ) and Delta (δ) angle

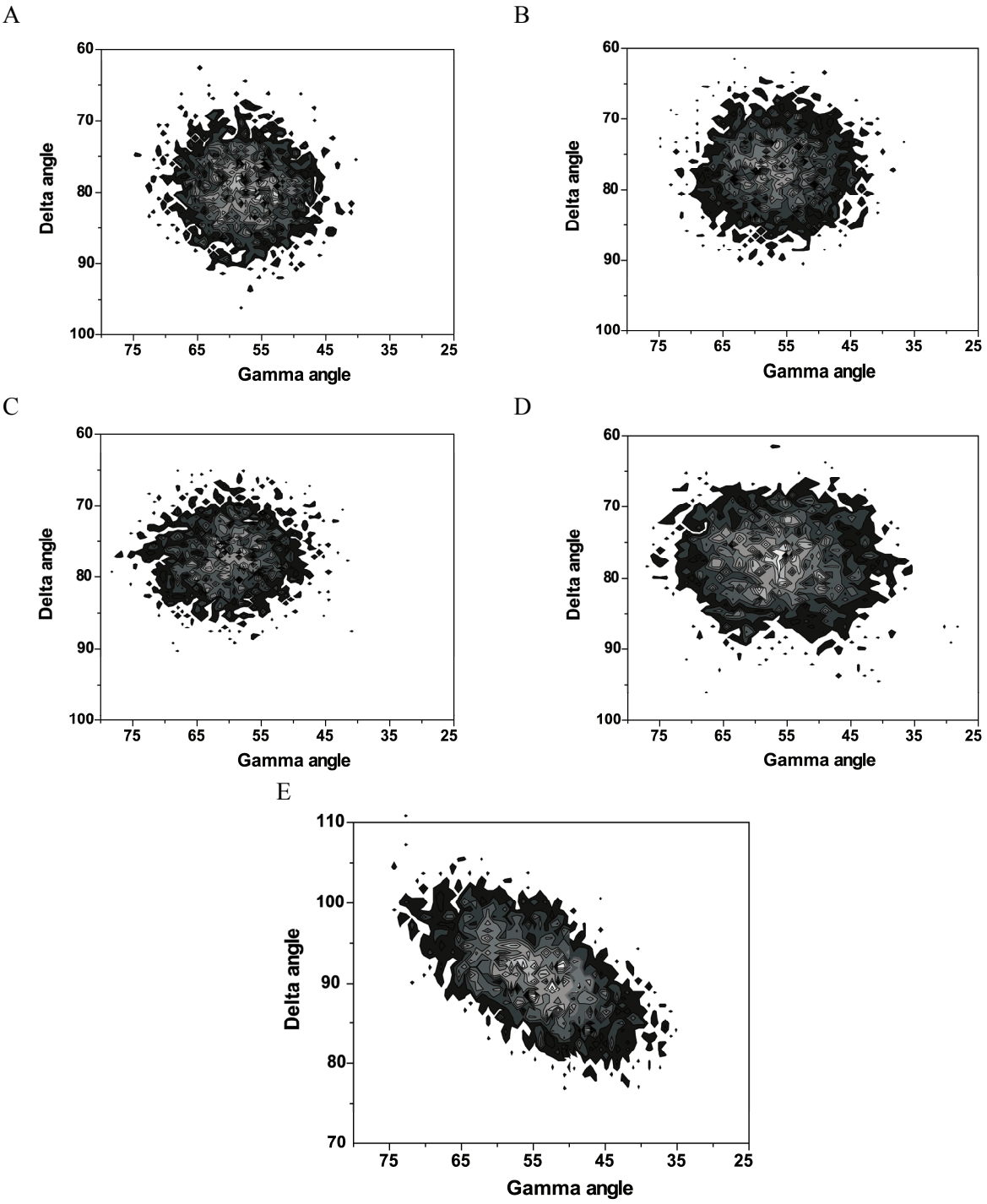

Figure S9. Population density map of the two dihedral angles gamma and delta plotted against each other over the 70 ns of MD simulation: (A) 2'-OH, (B) 2'-OMe, (C) 2'-F, (D) 4'-AM-2'-F, and (E) 4'-AM-2'-OMe uridine. Increasing color contrasts from white to black indicate the decrease in the populations of sugar dihedrals.

Population density map of Epsilon (ε) and Zeta (ζ) angle

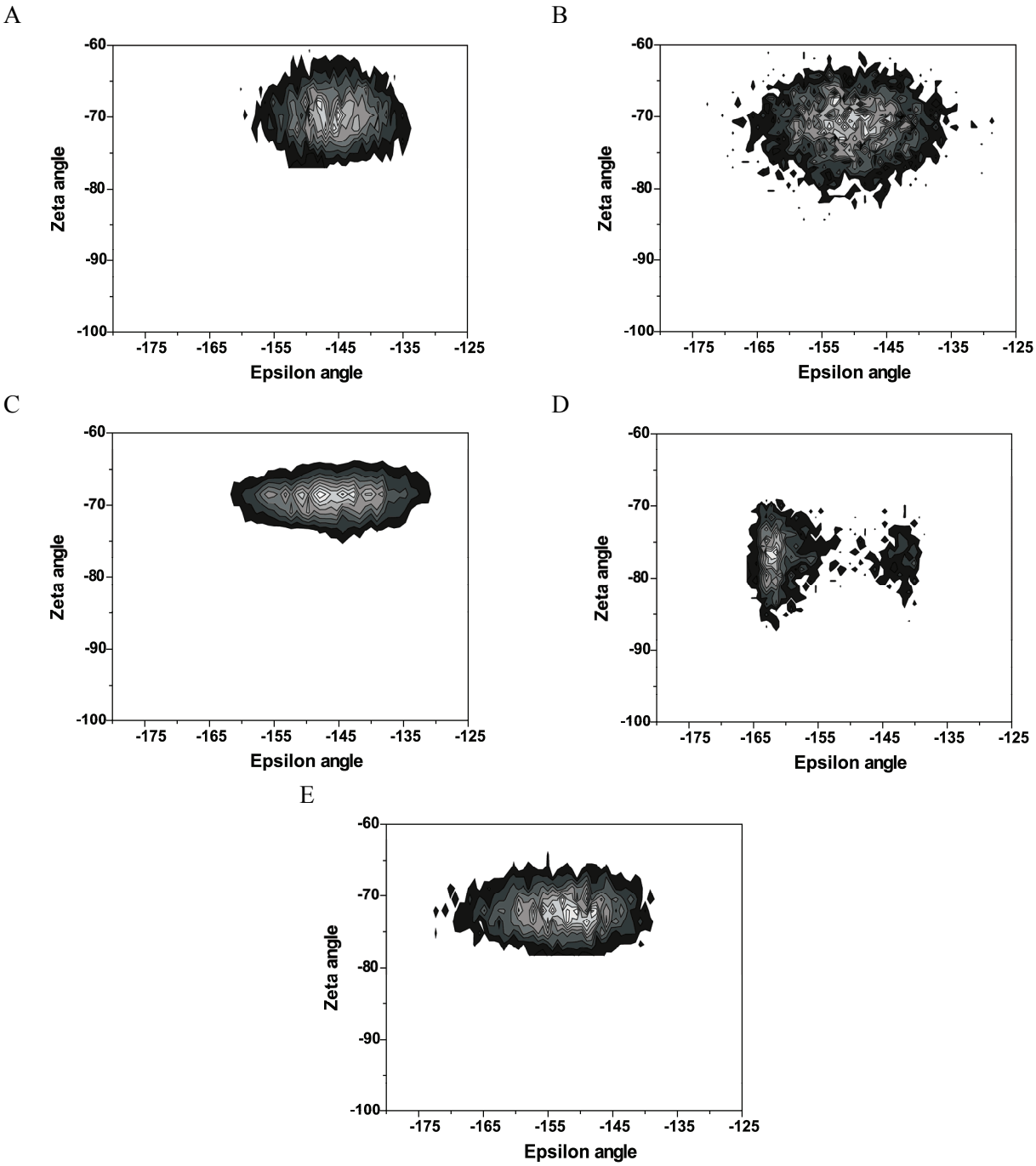

Figure S10. Population density map of the two dihedral angles the epsilon and zeta angle plotted against each other over the 70 ns of MD simulation: (A) 2'-OH, (B) 2'-OMe, (C) 2'-F, (D) 4'-AM-2'-F, and (E) 4'-AM-2'-OMe uridine. Increasing color contrasts from white to black indicate the decrease in the populations of sugar dihedrals.

Structures at m_1 for modified and unmodified uridines

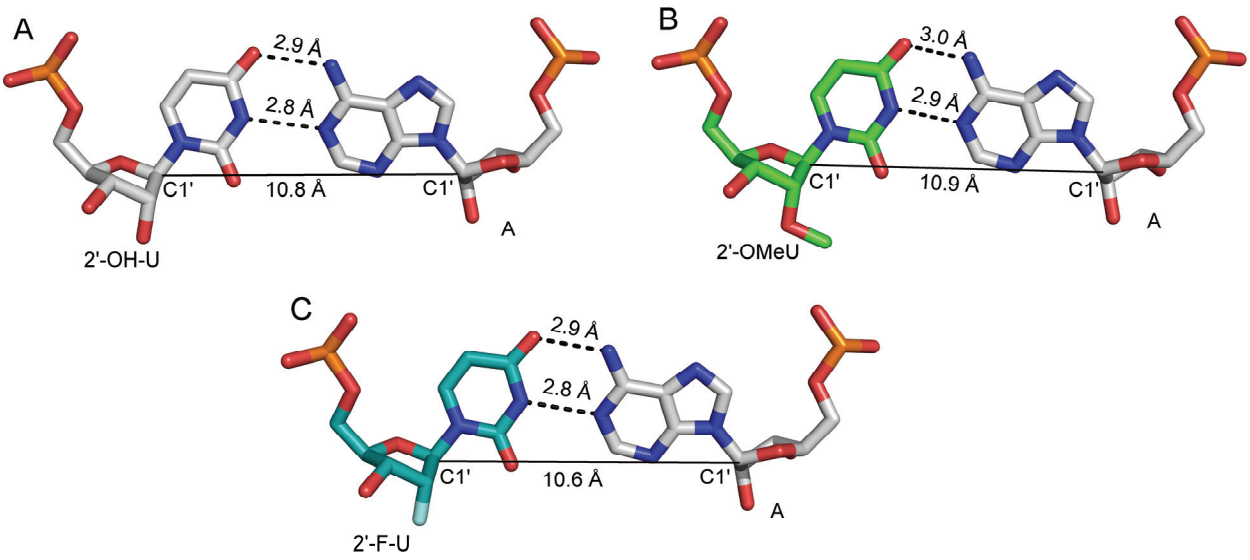

Figure S11. MD snapshot at m_1 (Figure 4, main text) of modified base pairs from the 35 ns of umbrella sampling simulations. The sugar conformation of modified and unmodified uridine nucleotides: (A) 2'-OH ($\Delta G°$ −4.51 kcal/mol), (B) 2'-OMe ($\Delta G°$ −4.47 kcal/mol) and (C) 2'-F ($\Delta G°$ −4.83 kcal/mol) are represented with base pairing adenosine.[6] Black dotted line represents the H-bond and their distances between the nitrogenous bases are shown in Å. The solid line represents the distance between C1'-C1' of the U-A base pair. The $\Delta G°$ values are free energies of Watson and Crick H-bonds.

Hydration of grooves at m_1 from umbrella sampling simulations

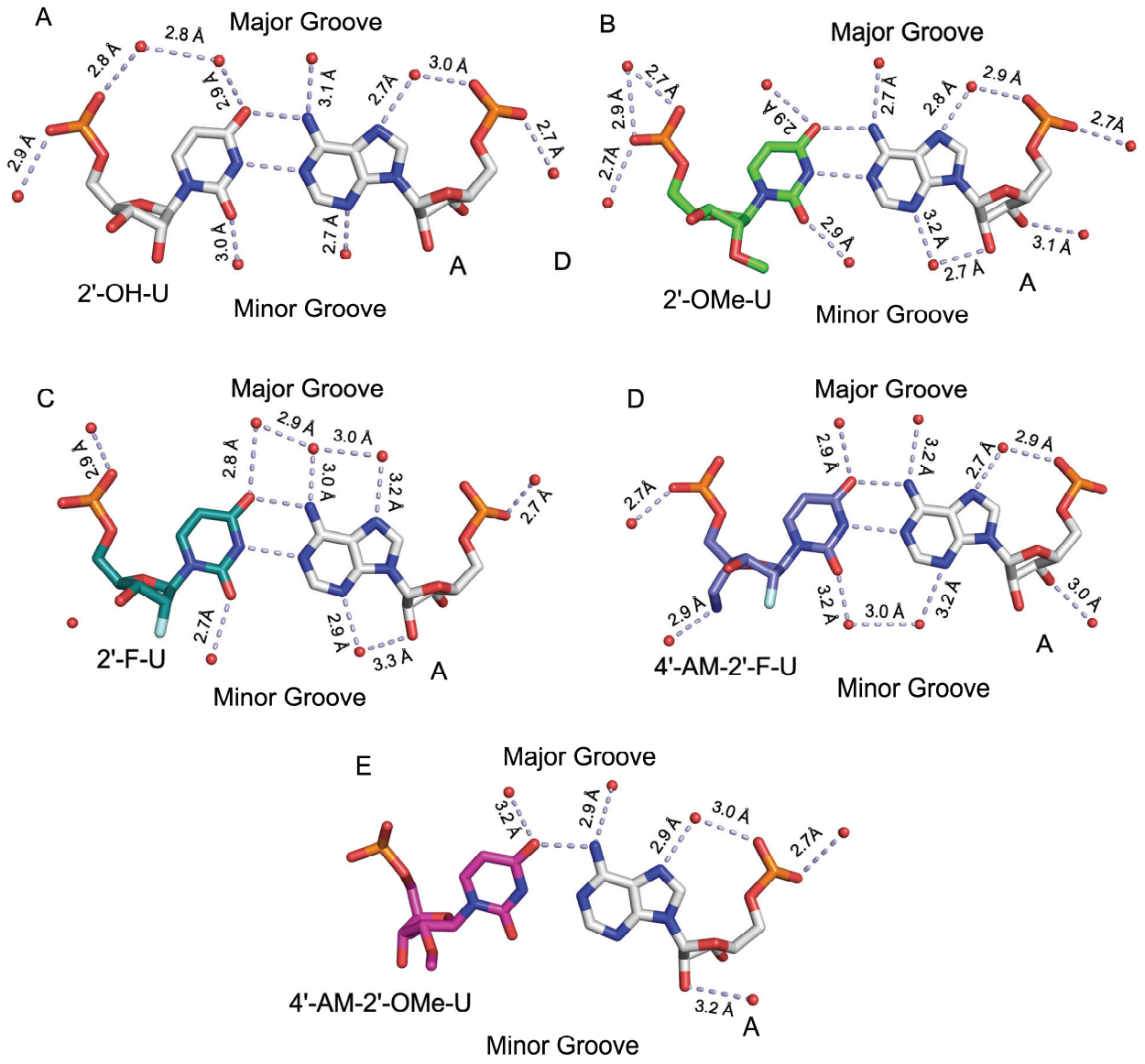

Figure S12. The hydration of base pairs in the minor and major groove of modified and unmodified RNAs: (A) 2'-OH, (B) 2'-OMe, (C) 2'-F, (D) 4'-AM-2'-F and (E) 4'-AM-2'-OMe. Red spheres indicate the presence of water molecule and dotted lines represent the interaction with the bases.

Frequency distribrution of χ from umbrella sampling simulations

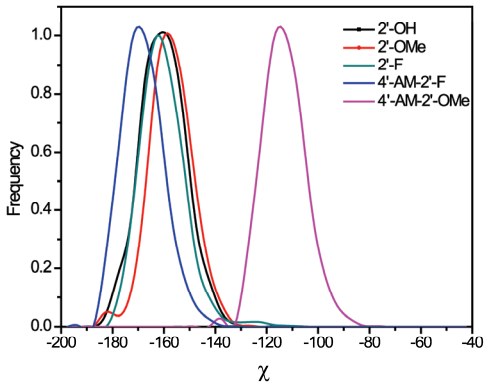

Figure S13. Frequency distribrution of χ over 35 ns of MD simulation in the unmodified, 2'-OMe, 2'-F, 4'-AM-2'-F, and 4'-AM-2'-OMe uridines.[7]

Energy optimized structure of 2'-F uridine

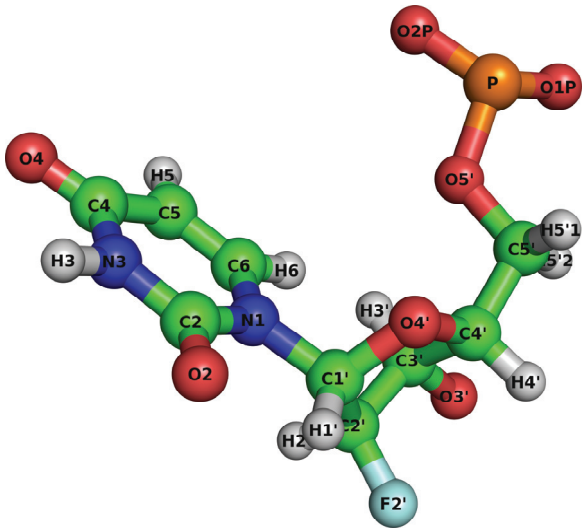

Atom Name	ESP Charge	Atom Name	ESP Charge
P	1.087840	C4	0.602236
O1P	−0.766660	O4	−0.565213
O2P	−0.766660	C5	−0.313528
O5'	−0.472500	C6	−0.213957
C5'	0.128940	H6	0.255733
H5'1	0.042562	H5	0.169741
H5'2	0.042562	H3	0.308704
C4'	0.152612	H1'	0.041659
O4'	−0.336190	H4'	0.039420
C1'	0.368621	C3'	0.067491
C2'	0.040453	O3'	−0.487823
F2'	−0.231410	H4'	0.146001
H2'	0.090331		
N1	0.111018		
C2	0.453877		
O2	−0.540735		
N3	−0.368045		

Figure S14. Energy optimized geometry and calculated RESP charges for 2'-F uridine using HF/6-31G* basis set in Gaussian 09 program. New force field parameters are generated using protocol developed by Kollman and co-workers.[3,4]

Energy optimized structure of 4'-AM-2'-F uridine

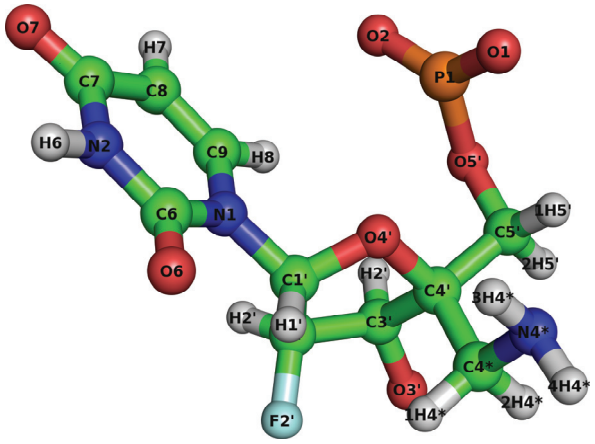

Atom Name	ESP Charge	Atom Name	ESP Charge
P	1.087840	C4	0.602236
O1P	−0.766660	O4	−0.565213
O2P	−0.766660	C5	−0.313528
O5'	−0.472500	C6	−0.213957
C5'	0.128940	H6	0.255733
H5'1	0.042562	H5	0.169741
H5'2	0.042562	H3	0.308704
C4'	0.152612	H1'	0.041659
O4'	−0.336190	C4*	0.025248
C1'	0.368621	1H4*	0.035965
C2'	0.040453	2H4*	0.035965
F2'	−0.291610	N4*	−1.012689
H2'	0.090331	3H4*	0.395855
N1	0.111018	4H4*	0.395855
C2	0.453877		
O2	−0.540735		
N3	−0.368045		

Figure S15. Energy optimized geometry and calculated RESP charges for 4'-AM-2'-F uridine using HF/6-31G* basis set in Gaussian 09 program. New force field parameters are generated using protocol developed by Kollman and co-workers.[3,4]

Sugar phosphate backbone torsions from DFT calculations

Modification	α	β	γ	δ	ε	ζ
2'-OH	–62.85	168.86	53.66	84.38	–157.53	–69.75
2'-OMe	–64.37	169.27	49.74	85.61	–152.25	–73.48
2'-F	–63.25	176.73	55.26	85.48	–149.31	–74.29
4'-AM-2'-F	–63.22	164.76	51.85	86.32	–151.84	–79.67
4'-AM-2'-OMe	–62.28	159.29	35.45	109.55	–137.24	–90.57

Table S1. Sugar phosphate backbone dihedral angles of unmodified and modified uridines from DFT calculations. The values are obtained during the potential energy scan at PBE density functional, 6-311++G* basis set in Gaussian 09 using PCM as solvent model. All the values are report in degree.

Sugar endocyclic torsions and sugar puckering derived from DFT calculations

Modification	ν_0	ν_1	ν_2	ν_3	ν_4	*P*	Puckering
2'-OH	4.7	−31.3	44.1	−40.5	22.6	13.5	C3'-endo
2'-OMe	4.9	−26.1	38.8	−36.5	18.9	11.6	C3'-endo
2'-F	4.2	−31.1	44.7	−43.1	24.5	14.2	C3'-endo
4'-AM-2'-F	7.2	−24.3	45.8	−49.6	33.6	24.8	C3'-endo
4'-AM-2'-OMe	−17.6	34.2	−36.4	26.2	−5.3	171.5	C2'-endo

Table S2. Sugar endocyclic torsional values exhibited by the different modifications and their pseudo rotational phase angle *(P)* values with puckering preferences. Endocyclic torsional angles are ν_0 (C4'-O4'-C1'-C2'), ν_1 (O4'-C1'-C2'-C3'), ν_2 (C1'-C2'-C3'-C4'), ν_3 (C2'-C3'-C4'-O4') and ν_4 (C3'-C4'-O4'-C1'). The values are obtained from the low energy conformations of each modification in solvent phase at PBE density functional at 6-311++G* basis set.

Sugar phosphate backbone torsion angle values from MD simulations

Modification	α	β	γ	δ	ε	ζ
2'-OH	−66.4	165.8	54.2	85.2	−152.4	−70.4
2'-OMe	−70.6	163.7	52.1	87.2	−155.4	−72.5
2'-F	−71.7	160.5	52.3	83.7	−158.3	−69.3
4'-AM-2'-F	−73.4	164.8	56.1	86.9	−154.2	−74.2
4'-AM-2'-OMe	−61.8	162.2	40.2	103.1	−140.8	−90.4

Table S3. Sugar phosphate backbone torsional angle values from the low energy conformations of 70 ns MD simulations. All the values are reported in degree.

Parameters used for umbrella sampling simulations of 2'-OH uridine

Run No	Minimum distance (Å)	Maximum distance (Å)	Size of the water box (Å)	No. of water molecules	Cut off (Å)	Simulation time (ps)	Production run (ns)
1	2.83	9.41	10	1767	10	30	
2	2.81	8.28	10	1769	10	30	
3	3.07	9.31	9	1715	10	30	
4	6.79	2.73	7	1695	10	45	7*5 = 35
5	7.73	2.90	8	1647	12	35	
6	9.18	2.81	8	1651	12	50	
7	2.74	9.47	10	1774	12	50	

Table S4. MD parameters used for the free energy error calculations of 35 ns umbrella sampling simulations. The error values were determined by carrying out MD simulations with different values of the minimum and maximum separation distances between bases within a model containing unmodified uridine.

Parameters used for umbrella sampling simulations of 2'-OMe uridine

Run No	Minimum distance (Å)	Maximum distance (Å)	Size of the water box (Å)	No. of water molecules	Cut off (Å)	Simulation time (ps)	Production run (ns)
1	2.80	9.35	9	1733	12	40	
2	2.80	8.47	10	1752	10	40	
3	3.03	9.38	10	1701	12	35	
4	6.81	2.79	8	1684	10	45	7*5 = 35
5	7.95	2.81	10	1673	12	30	
6	9.20	2.65	8	1647	12	60	
7	2.39	9.39	10	1789	10	45	

Table S5. MD parameters used for the free energy error calculations of 35 ns umbrella sampling simulations. The error values were determined by carrying out MD simulations with different values of the minimum and maximum separation distances between bases within a model containing 2'-OMe uridine.

Parameters used for umbrella sampling simulations of 2'-F uridine

Run No	Minimum distance (Å)	Maximum distance (Å)	Size of the water box (Å)	No. of water molecules	Cut off (Å)	Simulation time (ps)	Production run (ns)
1	2.86	9.25	9	1751	12	30	
2	2.88	8.39	10	1771	12	35	
3	3.09	9.44	10	1738	10	45	
4	6.84	2.75	10	1686	12	60	7*5 = 35
5	7.97	2.86	8	1664	10	60	
6	9.43	2.69	8	1658	10	50	
7	2.85	9.67	10	1784	10	50	

Table S6. MD parameters used for the free energy error calculations of 35 ns umbrella sampling simulations. The error values were determined by carrying out MD simulations with different values of the minimum and maximum separation distances between bases within a model containing 2'-F uridine.

Parameters used for umbrella sampling simulations of 4'-AM-2-F uridine

Run No	Minimum distance (Å)	Maximum distance (Å)	Size of the water box (Å)	No. of water molecules	Cut off (Å)	Simulation time (ps)	Production run (ns)
1	2.78	9.36	8	1760	10	50	
2	2.64	8.82	9	1781	12	40	
3	3.12	9.49	9	1743	10	45	
4	6.56	2.63	10	1672	12	60	7*5 = 35
5	7.84	2.76	8	1669	10	50	
6	9.56	2.52	9	1645	10	50	
7	2.76	9.86	10	1790	12	50	

Table S7. MD parameters used for the free energy error calculations of 35 ns umbrella sampling simulation. The error values were determined by carrying out MD simulations with different values of the minimum and maximum separation distances between bases within a model containing 4'-AM-2'-F uridine.

Parameters used for umbrella sampling simulations of 4'-AM-2'-OMe uridine

Run No	Minimum distance (Å)	Maximum distance (Å)	Size of the water box (Å)	No. of water molecules	Cut off (Å)	Simulation time (ps)	Production run (ns)
1	2.89	9.36	10	1758	10	35	
2	2.85	8.25	10	1764	10	30	
3	3.05	9.37	9	1720	10	30	
4	6.82	2.82	8	1695	12	50	7*5 = 35
5	7.95	2.91	7	1658	12	45	
6	9.22	2.75	7	1653	10	45	
7	2.87	9.54	10	1789	12	50	

Table S8. MD parameters used for the free energy error calculations of 35 ns umbrella sampling simulation. The error values were determined by carrying out MD simulations with different values of the minimum and maximum separation distances between bases within a model containing 4'-AM-2'-OMe uridine.

Free energy error calculations for umbrella sampling simulations

Run No	2'-OH	2'-OMe	2'-F	4'-AM-2'-F	4'-AM-2'-OMe
1	−4.46	−4.36	−4.77	−4.25	−3.14
2	−4.56	−4.25	−4.91	−3.98	−2.57
3	−4.38	−4.11	−4.75	−4.21	−2.13
4	−4.49	−4.15	−4.68	−4.11	−2.16
5	−4.19	−4.38	−5.22	−3.86	−2.39
6	−4.62	−4.05	−4.63	−4.38	−2.25
7	−4.57	−4.52	−4.58	−4.08	−2.39
Mean	−4.46	−4.26	−4.79	−4.12	−2.44
S. D.	±0.14	±0.16	±0.21	±0.17	±0.24

Table S9. Free energy error calculation for the umbrella sampling simulations. The error values were determined for the 35 ns of umbrella sampling simulations with different values of minimum and maximum base pair H-bond distance. All the values are represented in kcal/mol

References

1. Hendrickx, P. M. S.; Martins, J. C. *Chem. Cent. J.* **2008**, *2*, 20−27.
2. Contreras-García, J.; Johnson, E. R.; Keinan, S.; Chaudret, R.; Piquemal, J.-P.; Beratan, D. N.; Yang, W. *J. Chem. Theory Comput.* **2011**, *7*, 625−632.
3. Cornell, W.; Cieplak, P.; Bayly, C.; Gould, I.; Merz, K. J.; Ferguson, D.; Spellmeyer, D.; Fox, T.; Caldwell, J.; Kollman, P. *J. Am. Chem. Soc.* **1995**, *117*, 5179– 5197.
4. Aduri, R.; Psciuk, B. T.; Saro, P.; Taniga, H.; Schlegel, H. B.; SantaLucia, J. *J. Chem. Theory Comput.* **2007**, *3*, 1464–1475.
5. Perez, A.; Marchan, I.; Svozil, D.; Sponer, J.; Cheatham III, T. E.; Laughton, C. A.; Orozco, M. *Biophys. J.* **2007**, *92*, 3817–3826.
6. Patey G. N.; Valleau J. P. *J. Chem. Phy.* **1975**, *63*, 2334–2339.
7. Yildirim, I.; Stern, H. A.; Kennedy, S. D.; Tubbs, J. D.; Turner, D. H. *J. Chem. Theory Comput.* **2010**, *6*, 1520–1531.

NMR spectra (^{1}H, ^{13}C, & ^{19}F) (G- Grease, I- Impurity)

^{1}H NMR spectrum of compound **3**

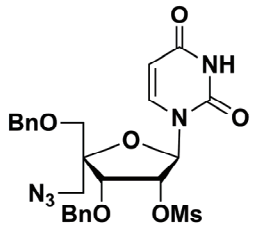

3

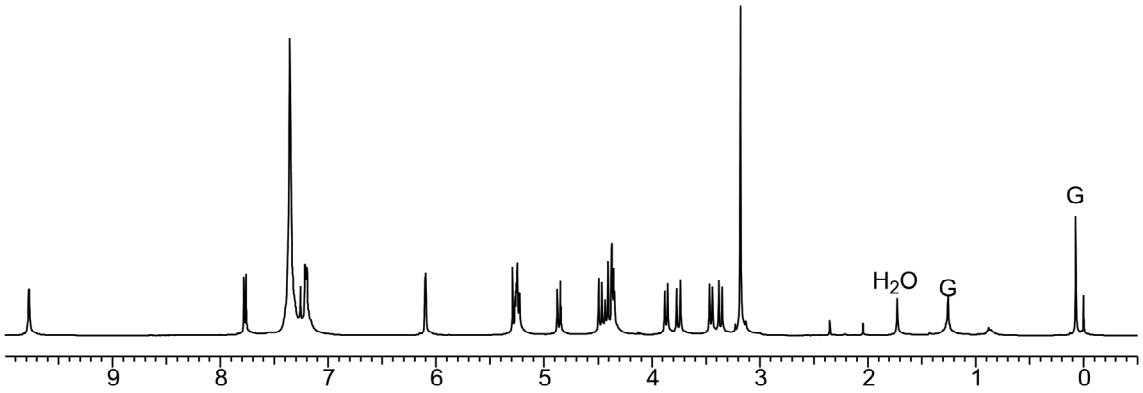

^{13}C NMR spectrum of compound **3**

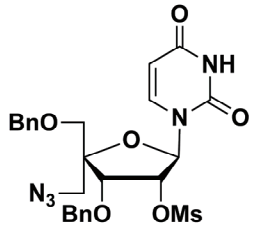

3

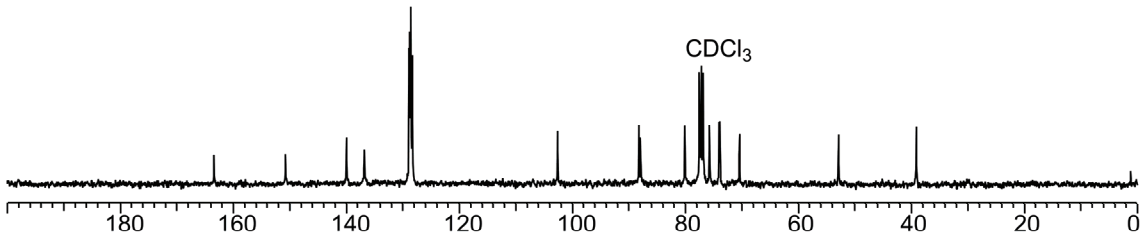

^{1}H NMR spectrum of compound **4**

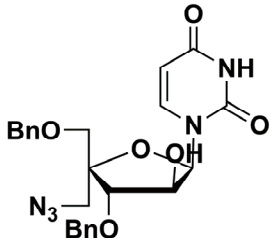

4

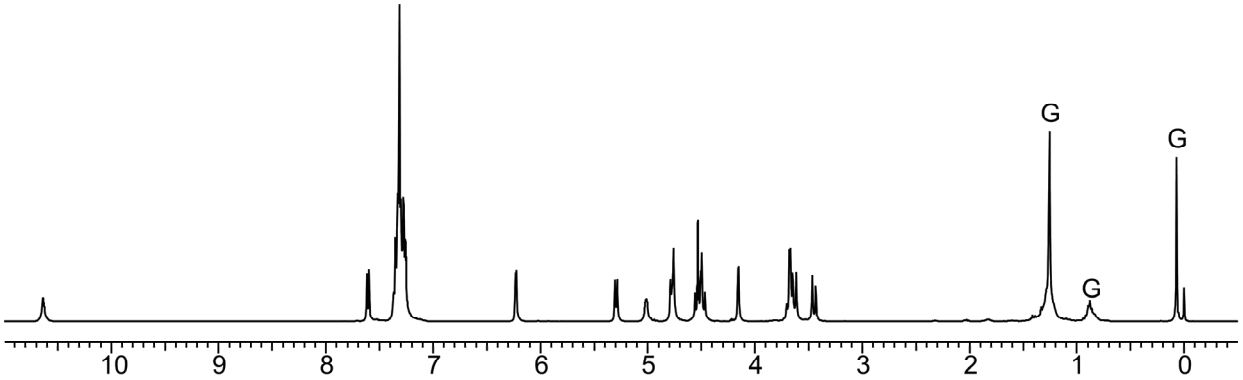

^{13}C NMR spectrum of compound **4**

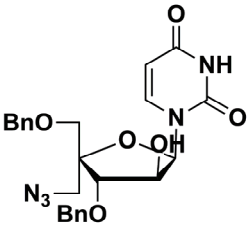

4

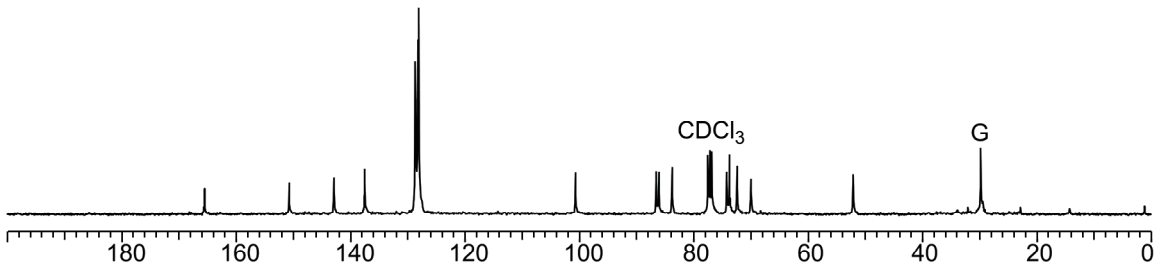

^{1}H NMR spectrum of compound **6**

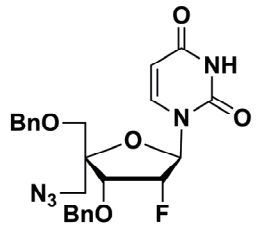

6

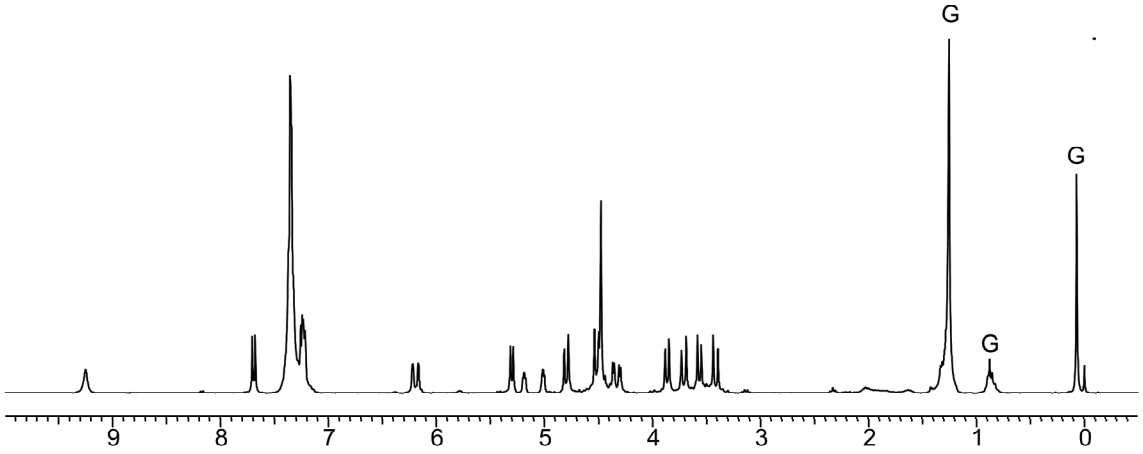

^{13}C NMR spectrum of compound **6**

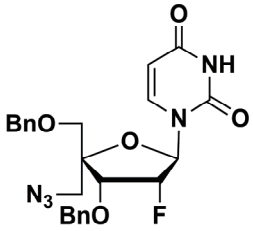

6

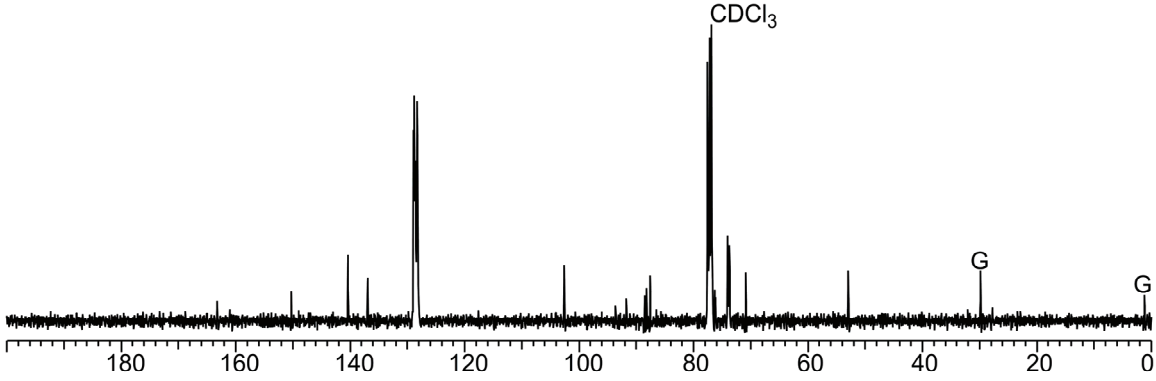

^{19}F NMR spectrum of compound **6**

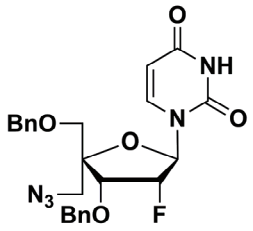

6

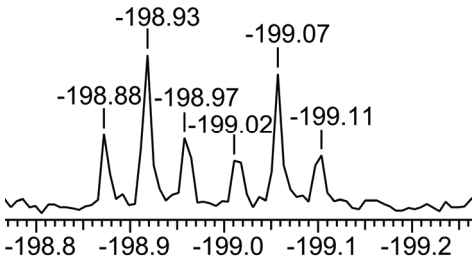

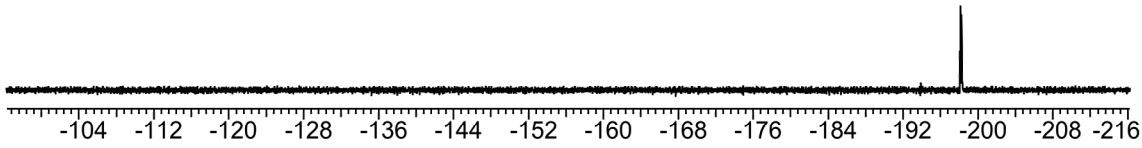

^{1}H NMR spectrum of compound **7**

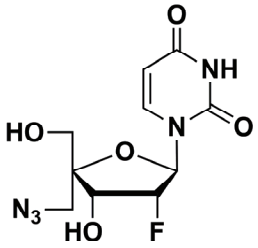

7

^{13}C NMR spectrum of compound **7**

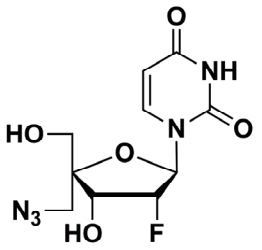

7

^{19}F NMR spectrum of compound **7**

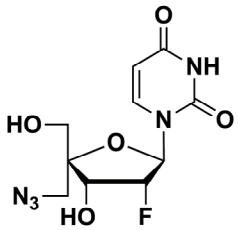

7

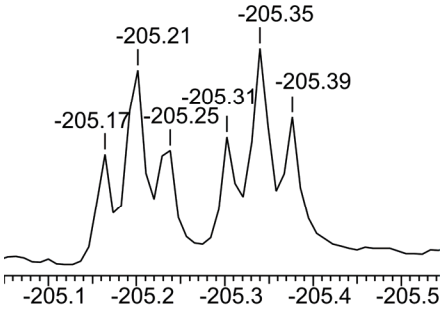

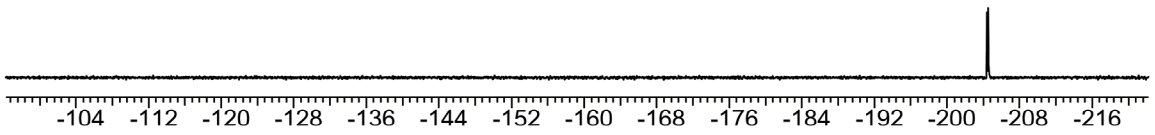

^{1}H NMR spectrum of compound **8**

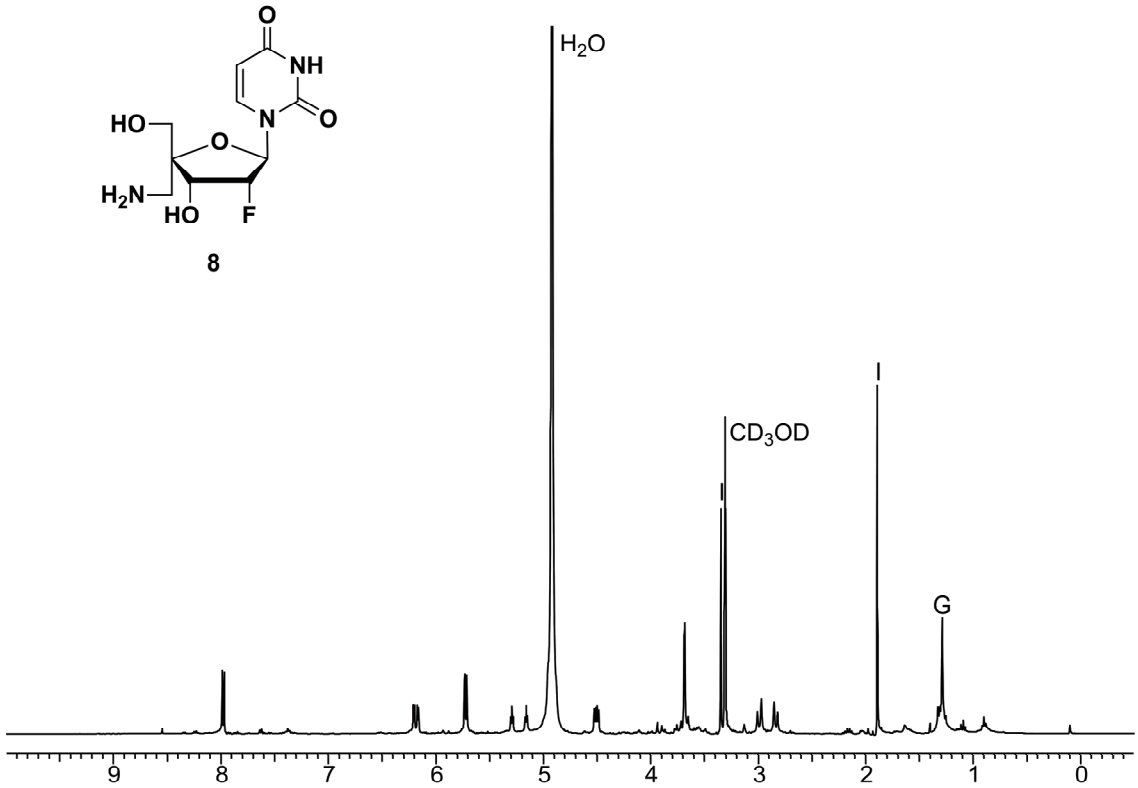

^{13}C NMR spectrum of compound **8**

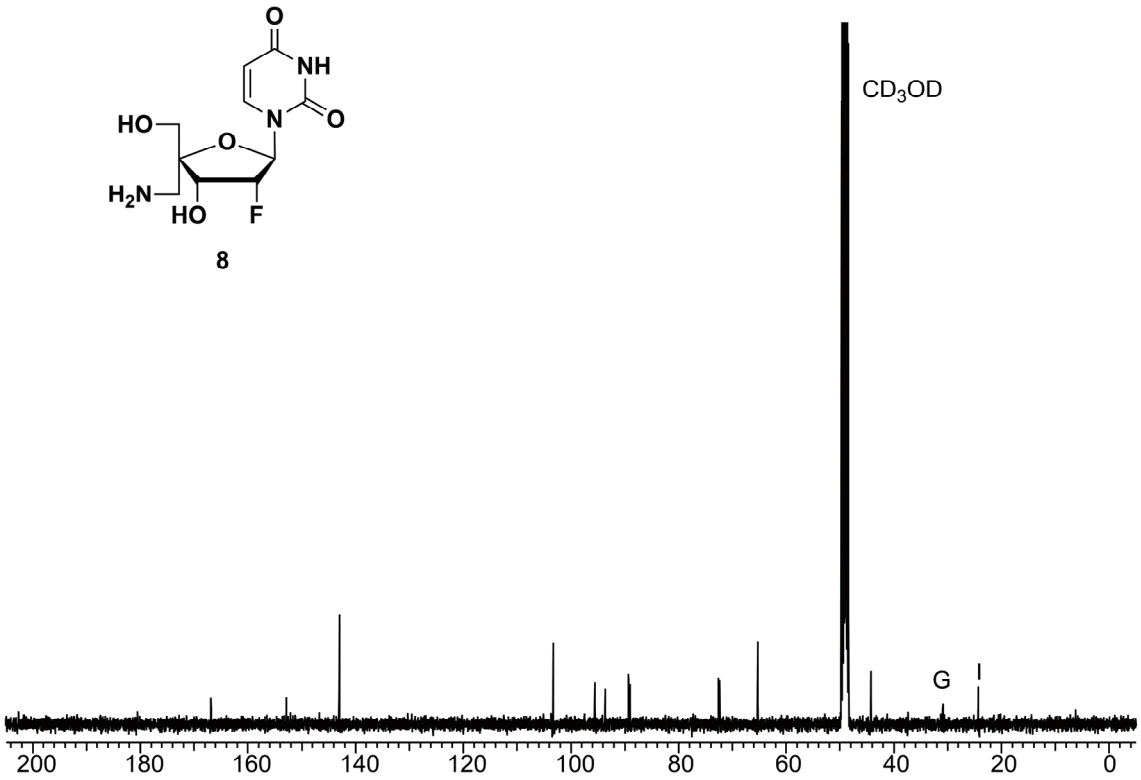

^{19}F NMR spectrum of compound **8**

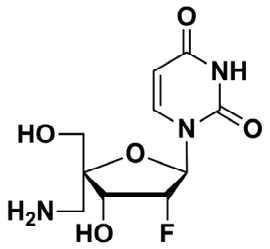

8